Supplementary Information for

The Two Enantiomers of Citalopram Bind to the human Serotonin Transporter in Reversed Orientations.

Heidi Koldsø[¶], Kasper Severinsen[‡], Thuy Tien. Tran[¶], Leyla Celik[§,¶], Henrik Helligsø Jensen[¶], Ove Wiborg[,‡], Birgit Schiøtt[*,§,¶], Steffen Sinning[‡]*

[§]Center for Insoluble Protein Structures (inSPIN), Interdisciplinary Nanoscience Center (iNANO), [¶]Department of Chemistry, University of Aarhus, Langelandsgade 140, DK-8000 Aarhus C, Denmark. [‡]Laboratory of Molecular Neurobiology, Centre for Psychiatric Research, Aarhus University Hospital, Risskov, Denmark.

The Supplementary Information is organized as follows. First, in Table S1 and S2 computed scores from the docking simulations, distances, and angles are listed for all poses using IFD and QPLD of *S*- and *R*-citalopram in wt hSERT, respectively, are listed. Next, the supplementary methods section provides details of the molecular modeling study including calculated partial charges in the QPLD calculations (Table S3) and docking in the S2-site (Table S4) along with synthesis of the citalopram analogs. Finally, physical data for the optical pure substrates (Table S5) and NMR spectra of the pure compounds are given.

Table S1: Computed scores, distances, and angles for all poses of *S*-citalopram. Angle 1 and 2 refer to the two dihedral angles of the propylamine group. [a] Only contributions from the XP scoring are included here. The RMSD values are calculated "in place" relative to the minimized reference structure in each cluster (the one used for QPLD input). The RMSD is calculated between the furan oxygen, the fluoro group, the positively charged tertiary ammonium nitrogen, and cyano nitrogen atoms, respectively.

Cluster	Method	Scorings Function	GlideScore (kcal/mol)	Emodel (kcal/mol)	Prime Energy (kcal/mol)	IFDScore (kcal/mol)	Distance Asp98(Oδ)-N^+ (Å)	Angle 1 (°)	Angle 2 (°)	RMSD S1 (Å)	RMSD S2 (Å)
S-Cluster0	IFD	SP/XP	-12.6	-74.2	-17055.4	-865.4	4.18	79.66	103.30	5.36	7.93
S-Cluster0	IFD	SP/XP	-11.4	-13.8	-17029.2	-862.9	2.75	157.65	-109.49	6.92	3.68
S-Cluster0	IFD	SP/XP	-10.8	-66.1	-17058.7	-863.7	3.83	108.59	144.25	7.82	5.93
Mean			**-11.6[a]**	**-51.4**	**-17047.8**	**-864.0**	**3.59**	**115.30**	**46.02**	**6.70**	**5.85**
Stdv			**0.9[a]**	**32.8**	**16.2**	**1.3**	**0.75**	**39.42**	**136.22**	**1.24**	**2.13**
S-ClusterI	IFD	SP/XP	-9.7	-17.0	-17039.1	-861.6	4.78	72.77	73.95	1.54	8.00
S-ClusterI	IFD	SP/XP	-9.3	-16.1	-17031.5	-860.9	4.91	64.77	82.10	1.28	7.83
S-ClusterI	QPLD	SP/SP	-8.9	-78.3			5.57	66.01	57.76	0.72	7.87
S-ClusterI	QPLD	SP/SP	-8.9	-76.6			5.49	66.12	56.46	0.73	7.87
S-ClusterI	QPLD	SP/SP	-8.7	-77.4			5.48	62.38	65.96	0.67	7.85
S-ClusterI	QPLD	SP/SP	-8.6	-77.5			5.54	60.31	70.61	0.66	7.85
S-ClusterI	QPLD	SP/XP	-8.4	-71.1			5.31	79.20	42.54	0.75	7.88
S-ClusterI	QPLD	SP/XP	-8.4	-68.4			5.29	76.07	41.05	0.75	7.86
S-ClusterI	QPLD	XP/XP	-8.4	-70.5			5.31	78.95	44.84	0.73	7.86
S-ClusterI	QPLD	SP/XP	-8.2	-69.4			5.31	93.08	27.24	0.82	7.88
S-ClusterI	QPLD	XP/XP	-8.1	-63.9			4.97	90.17	47.94	0.71	7.86
S-ClusterI	QPLD	SP/XP	-8.1	-66.7			5.35	80.21	44.40	0.80	7.86
S-ClusterI	IFD	SP/XP	-8.0	-66.2	-17054.5	-860.8	5.31	64.90	61.06	0.52	7.66
S-ClusterI	IFD	SP/XP	-8.0	-47.6	-17034.7	-859.7	4.49	61.10	81.99	1.87	7.82
S-ClusterI	QPLD	SP/XP	-7.9	-62.8			5.25	89.79	18.03	0.86	7.87
S-ClusterI	IFD	SP/XP	-7.8	-52.8	-17046.7	-860.1	4.10	63.50	80.49	0.92	7.80
S-ClusterI	QPLD	SP/XP	-7.6	-60.3			5.09	48.05	102.87	0.76	7.86
S-ClusterI	QPLD	SP/XP	-7.6	-59.3			5.34	59.25	91.24	0.83	7.88
S-ClusterI	QPLD	XP/XP	-5.4	-65.6			5.60	64.17	58.68	0.82	7.88
S-ClusterI	QPLD	SP/XP	-5.0	-67.5			4.99	53.23	99.61	0.80	7.85
S-ClusterI	QPLD	SP/XP	-4.6	-64.4			5.59	63.99	61.21	0.73	7.86
S-ClusterI	QPLD	SP/XP	-4.3	-60.0			5.41	102.70	16.60	0.71	7.89
S-ClusterI	QPLD	SP/XP	-3.8	-53.3			6.33	120.61	-148.97	0.83	7.92
S-ClusterI	QPLD	XP/XP	-1.8	-63.2			6.37	146.26	-106.76	0.87	7.90
Mean			**-7.0[a]**	**-61.0**	**-17041.3**	**-860.6**	**5.30**	**76.15**	**44.62**	**0.86**	**7.86**
Stdv			**2.1[a]**	**15.4**	**9.3**	**0.7**	**0.48**	**22.35**	**58.21**	**0.30**	**0.06**
S-ClusterII	QPLD	SP/XP	-11.1	-87.2			3.89	64.50	98.41	7.68	0.68
S-ClusterII	QPLD	SP/XP	-11.1	-88.5			3.89	64.90	98.75	7.69	0.69
S-ClusterII	QPLD	XP/XP	-11.0	-86.8			3.88	66.54	92.83	7.67	0.66
S-ClusterII	QPLD	XP/XP	-11.0	-88.9			3.89	65.85	93.80	7.66	0.68
S-ClusterII	QPLD	SP/XP	-11.0	-88.5			4.42	-70.54	-141.84	7.62	0.67
S-ClusterII	QPLD	SP/XP	-11.0	-85.8			4.56	-66.24	-151.30	7.59	0.66
S-ClusterII	QPLD	SP/XP	-11.0	-86.2			4.27	133.19	-57.50	7.65	0.73
S-ClusterII	QPLD	SP/XP	-10.9	-86.0			4.18	133.16	-64.01	7.64	0.72
S-ClusterII	QPLD	SP/XP	-10.9	-89.2			4.16	133.11	-69.63	7.63	0.72
S-ClusterII	QPLD	XP/XP	-10.9	-86.3			4.19	132.67	-65.67	7.65	0.69
S-ClusterII	QPLD	SP/XP	-10.9	-86.0			4.15	133.25	-68.34	7.65	0.71
S-ClusterII	QPLD	SP/XP	-10.9	-86.5			4.13	132.67	-70.73	7.65	0.69
S-ClusterII	QPLD	SP/XP	-10.9	-86.2			4.16	132.88	-68.92	7.65	0.69
S-ClusterII	QPLD	SP/XP	-10.9	-85.0			4.58	-69.19	-148.51	7.61	0.69

S-ClusterII	QPLD	SP/XP	-10.9	-87.2			4.52	-65.42	-144.87	7.60	0.72
S-ClusterII	IFD	SP/XP	-10.9	-82.9	-17034.2	-862.6	4.37	-66.17	-160.95	7.60	0.55
S-ClusterII	QPLD	XP/XP	-10.9	-88.3			4.37	-70.89	-137.37	7.62	0.68
S-ClusterII	QPLD	XP/XP	-10.9	-86.4			4.20	130.76	-70.27	7.61	0.68
S-ClusterII	QPLD	SP/XP	-10.8	-87.2			4.51	-69.99	-153.92	7.61	0.71
S-ClusterII	QPLD	XP/XP	-10.8	-85.5			4.14	131.86	-64.41	7.63	0.73
S-ClusterII	QPLD	XP/XP	-10.8	-86.4			4.10	136.59	-71.60	7.64	0.67
S-ClusterII	QPLD	SP/XP	-10.7	-85.0			4.18	126.00	-56.47	7.63	0.75
S-ClusterII	QPLD	SP/XP	-10.7	-85.1			4.13	137.09	-68.82	7.63	0.69
S-ClusterII	QPLD	SP/SP	-10.7	-103.8			4.51	-69.32	-152.09	7.61	0.69
S-ClusterII	QPLD	SP/SP	-10.6	-102.7			4.50	-67.37	-151.08	7.62	0.68
S-ClusterII	QPLD	SP/SP	-10.6	-103.1			4.51	-67.84	-150.84	7.62	0.71
S-ClusterII	QPLD	SP/XP	-10.6	-84.0			4.16	141.02	-79.23	7.64	0.71
S-ClusterII	QPLD	SP/XP	-10.6	-84.7			3.78	70.36	93.81	7.69	0.82
S-ClusterII	QPLD	SP/SP	-10.6	-103.7			4.50	-65.61	-151.12	7.62	0.68
S-ClusterII	QPLD	SP/SP	-10.5	-104.1			4.49	-69.30	-152.04	7.60	0.69
S-ClusterII	QPLD	XP/XP	-10.5	-83.8			4.24	78.51	46.06	7.68	0.93
S-ClusterII	QPLD	SP/SP	-10.5	-103.0			4.55	-68.03	-147.13	7.60	0.75
S-ClusterII	QPLD	SP/SP	-10.5	-101.8			4.55	-68.18	-147.79	7.62	0.70
S-ClusterII	QPLD	SP/SP	-10.5	-102.9			4.50	-67.92	-151.31	7.61	0.72
S-ClusterII	QPLD	SP/SP	-10.5	-102.9			4.53	-67.96	-150.81	7.59	0.72
S-ClusterII	QPLD	SP/SP	-10.4	-101.6			4.51	-69.41	-152.40	7.60	0.68
S-ClusterII	QPLD	SP/SP	-10.4	-96.3			4.42	-171.65	141.80	7.65	0.87
S-ClusterII	QPLD	SP/SP	-10.3	-96.0			4.27	-172.08	136.26	7.67	0.83
S-ClusterII	QPLD	SP/SP	-10.2	-89.5			4.43	-172.76	147.07	7.66	0.87
S-ClusterII	QPLD	SP/SP	-10.2	-95.4			4.35	-171.53	139.39	7.67	0.84
S-ClusterII	QPLD	SP/SP	-10.2	-90.1			4.47	-173.08	146.09	7.68	0.88
S-ClusterII	QPLD	SP/SP	-10.1	-92.2			4.39	-170.04	146.52	7.68	0.87
S-ClusterII	QPLD	SP/SP	-10.1	-94.4			4.37	-171.67	142.11	7.66	0.87
S-ClusterII	QPLD	SP/SP	-10.1	-93.9			4.37	-172.66	139.07	7.64	0.87
S-ClusterII	IFD	SP/XP	-10.1	-49.0	-17055.1	-862.8	3.57	-32.11	-159.72	7.62	0.38
S-ClusterII	QPLD	SP/SP	-10.1	-90.9			4.47	88.61	69.93	7.72	0.94
S-ClusterII	QPLD	SP/SP	-10.0	-93.9			4.44	87.45	56.87	7.67	0.84
S-ClusterII	QPLD	SP/XP	-9.9	-86.7			4.59	-69.73	-152.05	7.58	0.72
S-ClusterII	QPLD	SP/SP	-9.0	-62.4			4.91	51.27	-165.43	7.46	1.24
S-ClusterII	QPLD	SP/SP	-9.0	-58.7			4.90	-66.57	137.02	7.47	1.15
S-ClusterII	QPLD	SP/SP	-8.9	-58.3			4.92	-17.92	176.31	7.47	1.11
S-ClusterII	QPLD	SP/SP	-8.8	-58.3			4.83	-70.58	138.48	7.48	1.13
S-ClusterII	QPLD	SP/SP	-8.8	-60.2			5.29	-57.21	127.69	7.47	1.21
S-ClusterII	QPLD	SP/SP	-8.8	-56.6			4.98	-73.05	133.66	7.48	1.16
S-ClusterII	QPLD	SP/SP	-8.8	-56.0			5.03	2.89	170.82	7.49	1.09
S-ClusterII	QPLD	SP/SP	-8.8	-56.5			4.92	-67.36	138.04	7.49	1.15
S-ClusterII	QPLD	SP/SP	-8.8	-54.5			5.39	57.66	-154.02	7.49	1.24
S-ClusterII	QPLD	SP/SP	-8.7	-54.1			5.34	60.39	-147.23	7.48	1.20
S-ClusterII	QPLD	SP/SP	-8.6	-56.5			4.92	-61.97	137.29	7.49	1.15
S-ClusterII	QPLD	SP/SP	-8.6	-51.4			5.45	60.62	-149.01	7.49	1.21
S-ClusterII	QPLD	SP/SP	-8.6	-59.4			5.36	-52.05	125.62	7.48	1.18
S-ClusterII	QPLD	SP/SP	-8.6	-55.9			4.90	-1.80	168.98	7.48	1.09
S-ClusterII	QPLD	SP/SP	-8.6	-57.4			5.30	-49.52	132.82	7.48	1.23
S-ClusterII	QPLD	SP/SP	-8.5	-58.1			4.87	-17.83	168.76	7.48	1.06
Mean			**-10.8**[a]	**-82.1**	**-17044.6**	**-862.7**	**4.49**	**-9.67**	**-12.57**	**7.60**	**0.84**
Stdv			**0.3**[a]	**16.6**	**14.8**	**0.2**	**0.41**	**100.49**	**129.29**	**0.07**	**0.21**

Table S2 Computed scores, distances, and angles for all poses of *R*-citalopram. Angle 1 and 2 refer to the two dihedral angles of the propylamine group. [a] Only contributions from the XP scoring are included here. The RMSD values are calculated "in place" relative to the minimized reference structure in each cluster (the one used for QPLD input). The RMSD is calculated between the furan oxygen, the fluoro group, the positively charged tertiary ammonium nitrogen, and cyano nitrogen atoms, respectively.

Cluster	Method	Scorings Function	GlideScore (kcal/mol)	Emodel (kcal/mol)	Prime Energy (kcal/mol)	IFDScore (kcal/mol)	Distance Asp98(Oδ)-N^+ (Å)	Angle 1 (°)	Angle 2 (°)	RMSD R1 (Å)	RMSD R2 (Å)
***R*-Cluster0**	IFD	SP/XP	-9.9	-55.0	-17067.0	-863.3	4.99	-69.39	132.05	7.97	6.04
***R*-ClusterI**	QPLD	XP/XP	-8.9	-43.4			3.42	-70.74	170.77	1.28	7.94
***R*-ClusterI**	QPLD	SP/XP	-8.8	-38.4			3.25	-101.35	154.16	1.24	7.93
***R*-ClusterI**	QPLD	XP/XP	-8.8	-40.5			3.03	139.46	-70.92	1.20	7.97
***R*-ClusterI**	QPLD	SP/XP	-8.8	-36.4			2.99	140.18	-74.40	1.19	7.97
***R*-ClusterI**	QPLD	SP/XP	-8.8	-35.8			3.40	-71.40	167.72	1.29	7.95
***R*-ClusterI**	QPLD	XP/XP	-8.7	-42.0			3.27	132.10	-69.97	1.20	7.98
***R*-ClusterI**	IFD	SP/XP	-8.6	-37.2	-17030.1	-860.1	3.20	-90.12	153.51	1.40	7.66
***R*-ClusterI**	QPLD	SP/XP	-8.5	-37.1			3.20	136.37	-66.40	1.20	7.98
***R*-ClusterI**	QPLD	SP/XP	-8.5	-33.9			3.00	141.64	-80.45	1.18	7.98
***R*-ClusterI**	IFD	SP/XP	-8.3	-32.9	-17036.6	-860.2	4.35	141.03	-57.03	1.71	7.92
***R*-ClusterI**	QPLD	SP/SP	-8.3	-60.3			3.29	-74.92	170.17	1.25	7.95
***R*-ClusterI**	QPLD	SP/SP	-8.3	-57.7			3.31	-73.05	172.37	1.28	7.95
***R*-ClusterI**	IFD	SP/XP	-8.2	-32.2	-17029.2	-859.7	3.92	133.77	-77.31	1.48	7.92
***R*-ClusterI**	QPLD	SP/SP	-8.2	-61.5			3.16	127.76	-76.36	1.15	7.96
***R*-ClusterI**	QPLD	SP/SP	-8.2	-60.2			3.18	129.30	-73.76	1.15	7.97
***R*-ClusterI**	QPLD	SP/SP	-8.1	-60.8			3.02	138.92	-83.63	1.17	7.97
***R*-ClusterI**	QPLD	SP/SP	-8.1	-56.6			3.31	-72.80	172.56	1.26	7.95
***R*-ClusterI**	QPLD	SP/SP	-8.1	-54.1			3.31	-74.20	172.95	1.25	7.97
***R*-ClusterI**	QPLD	SP/SP	-8.0	-54.3			3.33	-79.01	167.79	1.27	7.94
***R*-ClusterI**	QPLD	SP/SP	-8.0	-55.8			3.34	-71.82	172.59	1.22	7.97
***R*-ClusterI**	QPLD	SP/SP	-8.0	-52.0			3.29	-74.34	169.40	1.27	7.95
***R*-ClusterI**	QPLD	SP/SP	-8.0	-33.7			3.41	-74.69	156.16	1.62	8.14
***R*-ClusterI**	QPLD	SP/SP	-8.0	-57.2			3.07	136.82	-77.17	1.17	7.98
***R*-ClusterI**	QPLD	SP/SP	-8.0	-53.8			3.28	-78.90	168.23	1.24	7.98
***R*-ClusterI**	QPLD	SP/SP	-8.0	-18.4			4.24	-97.05	175.10	1.20	8.08
***R*-ClusterI**	QPLD	SP/SP	-7.9	-20.5			4.23	-93.79	-173.61	1.22	8.08
***R*-ClusterI**	QPLD	SP/XP	-7.9	-40.8			3.36	-68.06	170.85	1.27	7.95
***R*-ClusterI**	QPLD	SP/SP	-7.9	-19.1			4.25	-94.73	-174.68	1.21	8.06
***R*-ClusterI**	QPLD	SP/SP	-7.9	-55.9			3.14	130.54	-77.45	1.15	7.98
***R*-ClusterI**	QPLD	SP/SP	-7.9	-51.3			3.34	-77.64	169.82	1.24	7.96
***R*-ClusterI**	QPLD	SP/SP	-7.8	-15.6			4.21	-96.01	-174.13	1.32	8.05
***R*-ClusterI**	QPLD	SP/SP	-7.8	-19.4			4.26	-90.85	-172.05	1.31	8.08
***R*-ClusterI**	QPLD	SP/SP	-7.8	-31.0			3.37	-69.40	159.23	1.67	8.15
***R*-ClusterI**	QPLD	SP/SP	-7.8	-49.0			3.33	-72.69	174.01	1.24	7.97
***R*-ClusterI**	QPLD	SP/SP	-7.7	-16.5			4.76	178.70	-154.53	1.44	8.09
***R*-ClusterI**	QPLD	SP/XP	-7.6	-39.0			3.10	137.37	-73.30	1.17	7.97
***R*-ClusterI**	QPLD	SP/XP	-7.5	-36.1			3.20	135.69	-66.40	1.19	7.99
***R*-ClusterI**	QPLD	SP/XP	-5.2	-22.2			4.73	88.37	74.96	1.45	8.10
***R*-ClusterI**	QPLD	SP/XP	-5.1	-16.4			4.64	87.05	81.86	1.40	8.09
***R*-ClusterI**	QPLD	SP/XP	-5.0	-20.4			4.72	87.54	74.58	1.47	8.07
Mean			**-7.8**[a]	**-40.0**	**-17032.0**	**-860.0**	**3.55**	**14.38**	**34.38**	**1.29**	**7.99**
Stdv			**1.4**[a]	**14.8**	**4.0**	**0.3**	**0.55**	**107.36**	**133.71**	**0.14**	**0.08**
***R*-ClusterII**	IFD	SP/XP	-10.2	-13.5	-17042.2	-862.3	4.66	49.05	-162.04	7.91	0.76
***R*-ClusterII**	IFD	SP/XP	-10.0	-13.9	-17041.9	-862.1	4.38	-95.06	146.95	8.06	0.79
***R*-ClusterII**	QPLD	SP/XP	-9.6	-26.2			4.60	38.35	-155.43	7.97	0.62

***R*-ClusterII**	QPLD	SP/XP	-9.5	-23.3			4.55	29.79	-142.34	7.95	0.65
***R*-ClusterII**	QPLD	SP/XP	-9.5	-22.6			4.65	35.88	-152.07	7.96	0.65
***R*-ClusterII**	QPLD	SP/XP	-9.5	-22.5			4.49	25.87	-149.97	7.96	0.63
***R*-ClusterII**	QPLD	XP/XP	-9.4	-23.0			4.44	14.99	-140.39	7.96	0.63
***R*-ClusterII**	QPLD	SP/XP	-9.4	-22.7			4.44	11.58	-134.93	7.95	0.64
***R*-ClusterII**	QPLD	SP/XP	-9.1	-30.3			3.31	-35.20	165.65	8.02	1.14
***R*-ClusterII**	QPLD	XP/XP	-9.0	-16.8			4.40	7.76	-125.53	7.93	0.66
***R*-ClusterII**	QPLD	SP/SP	-8.8	-40.8			4.65	41.07	-161.61	7.97	0.61
***R*-ClusterII**	QPLD	SP/SP	-8.7	-40.9			4.64	40.42	-162.42	7.98	0.61
***R*-ClusterII**	QPLD	SP/SP	-8.6	-37.6			4.71	43.43	-160.34	7.95	0.63
***R*-ClusterII**	QPLD	SP/SP	-8.6	-39.0			4.64	42.84	-160.70	7.97	0.60
***R*-ClusterII**	QPLD	SP/SP	-8.6	-39.7			4.64	40.54	-161.93	7.98	0.61
***R*-ClusterII**	QPLD	SP/SP	-8.5	-37.9			4.66	42.40	-160.48	7.97	0.61
***R*-ClusterII**	QPLD	SP/SP	-8.4	-35.8			4.68	42.11	-158.11	7.95	0.63
***R*-ClusterII**	QPLD	SP/XP	-8.4	-20.8			4.63	46.51	-150.82	7.92	0.90
***R*-ClusterII**	QPLD	SP/SP	-8.4	-52.7			3.27	-32.19	164.15	8.02	1.09
***R*-ClusterII**	QPLD	SP/SP	-8.4	-37.4			4.64	47.18	-162.73	7.96	0.63
***R*-ClusterII**	QPLD	SP/SP	-8.4	-37.2			4.64	42.34	-162.25	7.96	0.63
***R*-ClusterII**	QPLD	SP/SP	-8.3	-36.8			4.61	43.38	-164.20	7.96	0.61
***R*-ClusterII**	QPLD	SP/SP	-8.0	-34.8			4.72	66.65	-167.63	7.96	0.78
***R*-ClusterII**	QPLD	SP/SP	-7.9	-44.9			3.13	131.07	-81.47	8.10	0.79
***R*-ClusterII**	QPLD	SP/SP	-7.8	-33.9			4.78	70.17	-166.50	7.96	0.80
***R*-ClusterII**	QPLD	SP/SP	-7.8	-37.5			3.57	63.26	-172.81	8.07	0.97
***R*-ClusterII**	QPLD	SP/SP	-7.5	-34.3			3.39	135.45	-109.45	8.10	0.78
***R*-ClusterII**	QPLD	SP/SP	-7.4	-37.4			3.62	67.53	-161.26	8.07	1.07
***R*-ClusterII**	QPLD	SP/XP	-6.9	-21.6			4.68	55.76	-154.81	7.95	0.87
***R*-ClusterII**	QPLD	SP/XP	-5.9	-17.2			4.60	0.55	-134.21	7.93	0.87
***R*-ClusterII**	QPLD	XP/XP	-5.9	-18.4			4.67	-3.27	-123.80	7.91	0.89
***R*-ClusterII**	QPLD	SP/XP	-4.1	-26.1			4.54	59.92	-161.53	7.96	0.82
***R*-ClusterII**	QPLD	SP/XP	-3.9	-20.4			4.66	57.08	-163.51	7.96	0.79
Mean			**-8.1**[a]	**-28,2**	**-17042.0**	**-862.2**	**4.61**	**33.23**	**-142.72**	**7.96**	**0.70**
Stdv			**2.2**[a]	**9.2**	**0.2**	**0.1**	**0.10**	**31.63**	**59.19**	**0.03**	**0.10**

Supplementary Methods

Molecular Modeling

One homology model of hSERT has been used for IFD simulations in this study. This model has been extensively refined, as described below, compared to our previous homology model,[1] however mostly with respect to structural elements some distance away from the substrate binding site. The LeuT crystal structure was utilized as a template[2] and the employed alignment between hSERT and LeuT is based on the published refined alignment of neurotransmitter sodium symporters.[3] In addition to the crystal structure of LeuT, an optimized conformation of the extracellular loop 2 (EL2) connecting trans-membrane helices (TM) 3 and 4 has also been used as a template in building the model. This loop has been significantly refined compared to the one used previously.[1] EL2 contains some features that were not taken into consideration in the initial models; namely a disulfide bridge between Cys200 and Cys209[4,5] and an α-helix (residues Pro227-Leu237), as observed in the corresponding loop of LeuT. The presence of an α-helix in hSERT was supported by secondary structure prediction using the Jpred 3[6] and PSIPRED servers.[3,7] During validation of these loop models, the location of putative *N*-glycosylation sites[8] and proteolysis sites, analogous to the ones observed in hDAT,[9] were positioned to assure exposure to the aqueous phase.

Homology Modeling - All the loops in the original hSERT homology model[1] were first optimized using the loop model application in MODELLER 9v4.[10,11] During this process the disulfide bridge and additional secondary structure elements were incorporated in EL2. Secondly, the loops were examined visually to exclude broken or physically unlikely conformations and to fulfill the above-mentioned criteria of the features present. Thirdly, several validation methods, including the objective function[12] and Ramachandran plot using PROCHECK[13] and Verify 3D[14,15] were applied to differentiate between the models. Finally, the best resulting loop model was further optimized using the loop refinement tool as implemented in Prime[16] in the Schrödinger Suite 2008 package in

implicit solvent. The optimized loop was used as a template for EL2 in further refinement and building of a new homology model of hSERT. The remaining parts were aligned to the LeuT sequence according to Beuming *et al.*[3]

During the model building procedure of the full protein, 20 models were created and the best one was chosen on the basis of i) the cavity size measured in MVD, determined by the solvent accessible area method with a 1.2 Å probe,[17,18] ii) the probability density function,[12] iii) the Ramachandran plot,[13] and iv) the χ_1 angle of Asp98, which should be ±*gauche* to establish the sodium coordination as suggested by Yamashita *et al*.[2] This angle has previously been proposed to be approximately ±65º in homology models of hSERT with bound *S*-citalopram.[19] The employed model has 89.5, 8.5, 1.0, and 1.0 % populations in the most favorable, additionally allowed, generously allowed and disallowed regions, respectively. The five residues, Asn205(EL2), His240(EL2), Ala305(EL3), Met389(TM7), and Arg462(TM9) are in the disallowed region and the five residues Ser199(EL2), Asn211(EL2), Val397(EL4), Tyr572(TM12), and Ser574(TM12) are in the generously allowed region. All ten residues are located more than 12 Å away from the substrate in the binding pocket and is thus not expected to influence the binding site. The selected model had a volume of 114 $Å^3$.[17]

The two sodium ions identified in the LeuT crystal structure were manually included in the selected homology model with the same coordinates as in the pdb-structure (pdb-code: 2A65).[2] The chloride ion was furthermore manually placed in the proposed binding site.[20,21] The entire complex was then minimized with a conjugated gradient method for 10,000 steps in NAMD 2.6,[22] employing the CHARMM 27 protein force field[23] with the CMAP correction[24,25] to relieve any steric strain in the protein. Ultimately, the *C*-terminus was removed compared to the early homology model.[1] After refinement the resulting model contains a total of 536 residues ranging from Arg79 to Pro614. The final model is displayed in Figure S1 along with the knowledge included for modeling of EL2.

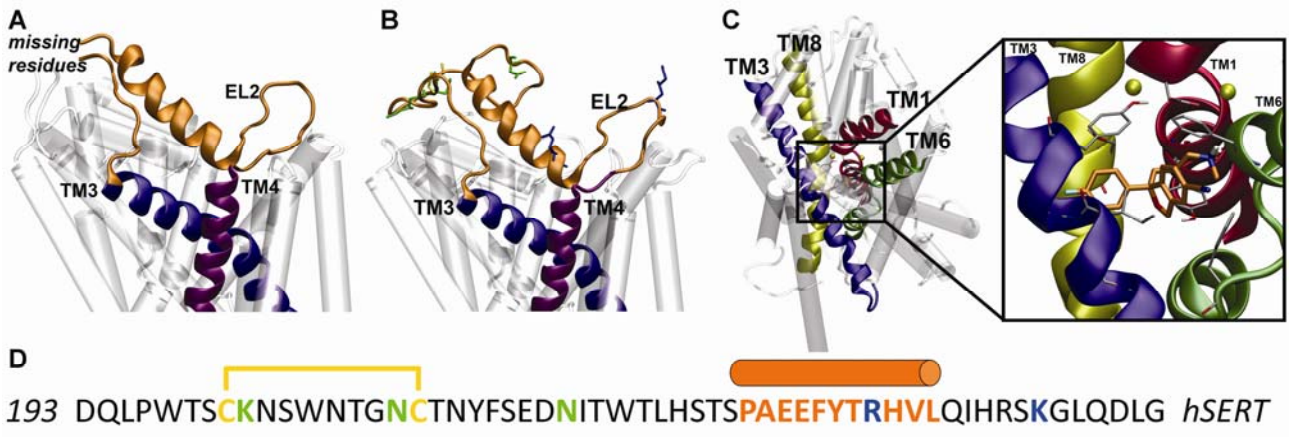

Figure S1. Refined homology model of hSERT built from the LeuT template. (**A**) The structure of LeuT[2] with focus on EL2 (orange) linking TM3 (purple) and TM4 (pink). (**B**) The refined model for hSERT is shown with glycosylation sites[8] in green, proteolysis sites[9] in blue, and the disulfide bridge[4,5] in yellow. (**C**) The full hSERT homology model displayed with *S*-citalopram (orange) inside the central cavity lined by TM1 (pink), TM3 (purple), TM6 (green) and TM8 (yellow). The two Na^+-ions are included as yellow spheres. (**D**) The experimental data included in EL2 modeling are indicated on the hSERT sequence of EL2; the disulfide bridge is marked in yellow, the α-helix in orange, glycosylation sites in green, and proteolysis sites in blue.

Ligand modeling - *S*- and *R*-citalopram (*S*-**1**, *R*-**1**) were built in Maestro.[26] The two enantiomers were minimized in the OPLS-AA force field[27] with and without implicit solvent until convergence using the conjugated gradient method in MacroModel 9.1 as implemented in the Schrödinger 2006 suite.[28] Furthermore, a Monte Carlo conformational search in vacuum was made in the OPLS-AA force field to identify all conformations within 50 kJ/mol of the lowest energy conformation. The conformation with lowest energy that did not include stabilizing intramolecular hydrogen bonds was chosen as the input structure for the IFDs. As a reference in the computation of internal strain of the bioactive conformations, the lowest energy conformation without an intramolecular hydrogen bond from an implicit water Monte Carlo simulation was applied according to the method by Boström *et al*.[29] The proton of the tertiary ammonium was found to have a pK_a value of 9.43 as

determined by Epik 1.6 implemented in the Schrödinger 2008 suite,[30] predicting the side chain amino group to be charged at physiological pH.

Protein preparation - The protein was further prepared for IFD by the use of the Protein Preparation Wizard in the Schrödinger 2008 suite (Schrödinger, LLC). The hydrogenation states were initially checked and optimized. The proposed protonation states were used in most of the cases; however, Asp524 and Glu508 were modeled as neutral on the basis of predictions by PROPKA 2.0[31]. The analogous position of Glu508 (Glu419) in the LeuT crystal structure has similarly been proposed to be protonated because of the close proximity to another acidic residue (Glu62).[20] A similar Glu-Glu (Glu508-Glu136) pair is also observed in this hSERT model giving rise to the protonation of Glu508. Ultimately, a restrained energy minimization was performed using the default settings. This minimization uses the OPLS-AA[27] force field and converges to a maximum RMSD of 0.3 Å. The refined protein structure was the input for the IFDs.

IFD - The two enantiomeric forms of citalopram were docked into the refined homology model of hSERT by means of IFD using Glide 5.0[32] and Prime 2.0[16] in Schrödinger Suite 2008. IFD introduces protein side chain flexibility in a radius of 5.0 Å around the poses from the initial soft docking stage.[33,34] The binding site for the initial docking was defined by five residues; Asp98, Ile172, Phe341, Thr439, and Gly442; all chosen based on biochemical results and previous binding models for 5-HT and imipramine in hSERT.[1,35] The residues chosen all line the central binding site also demonstrated by Celik *et al*,[1] some have been shown to be involved in interaction with bound ligands.[36-40] The IFD protocol applied uses the above mentioned residues as binding site definition; furthermore the box size used was 8.0Å x 8.0Å x 8.0 Å. The number of poses to keep in each Glide docking stage was set to 100, and the energy window was raised to 50 kcal/mol to allow for larger diversity in the output. The Standard Precision (SP) scoring function[41] was applied in the first Glide

docking stage and the Extra Precision (XP) scoring function[42] was employed in the final Glide re-docking stage.

QM-Polarized Ligand Docking (QPLD) - The selected binding pose of each cluster for each enantiomer generated from IFD were further evaluated by QPLD,[43] which is a combination of Glide and Qsite.[44] Because of the more precise treatment of the partial charges in QPLD, it is helpful for discriminating the proposed locations of the fluoro- and the cyano groups, which are those differing the most in the binding models. In the initial step, the QPLD protocol includes a Glide docking to produce unique ligand-protein complexes. QSite,[45] which is a QM/MM approach, then calculates partial atomic charges for the ligand with *ab initio* methods. In the last stage, a Glide re-docking is performed, using the optimized calculated partial charges of the ligand. The energetically most favorable poses are returned. An output of 20 poses was chosen to be returned from each QPLD calculation. The *Accurate* level was chosen for the QM implying a B3LYP/6-31G* level of theory for the QM treatment of the ligand.[43] Several setups of the QPLD have been tested (see Table 1 and S3) in order to explore the two scoring functions in Glide thoroughly. However, identical for all of them, the best ligand pose from the IFD concerning the GlideScore and Emodel is used to define the center in the grid generation step. The average value of the computed partial charges are found in Table S3.

Table S3. Average calculated partial charges of the atoms in the three functional groups of citalopram after QPLD docking. The charges in implicit water calculated at the same QM-level and in the IFD, force-field charges, are listed first for comparison. Numbers in brackets are computed standard deviations.

Cluster	Docking method	N^+	H_{NH}	C_{methyl}	H_{methyl}	N_{CN}	F
QM implicit water	**N/A**	0.08	0.36	-0.36 [0.04]	0.18 [0.01]	-0.53	-0.20
IFD	SP/XP	-0.02	0.21	0.09	0.06	-0.43	-0.22
***S*-ClusterI**	QPLD SP/SP	0.14 [0.00]	0.34 [0.01]	-0.50 [0.02]	0.22 [0.04]	-0.48 [0.00]	-0.16 [0.01]
	QPLD SP/XP	-0.01 [0.12]	0.36 [0.03]	-0.37 [0.26]	0.21 [0.04]	-0.47 [0.02]	-0.18 [0.01]
	QPLD XP/XP	0.09 [0.00]	0.45 [0.00]	-0.49 [0.07]	0.20 [0.04]	-0.48 [0.00]	-0.15 [0.00]
***S*-ClusterII**	QPLD SP/SP	0.09 [0.07]	0.33 [0.02]	-0.39 [0.08]	0.19 [0.03]	-0.39 [0.01]	-0.17 [0.01]
	QPLD SP/XP	0.08 [0.07]	0.34 [0.02]	-0.39 [0.08]	0.19 [0.03]	-0.39 [0.01]	-0.17 [0.00]
	QPLD XP/XP	0.15 [0.01]	0.34 [0.02]	-0.40 [0.04]	0.19 [0.02]	-0.39 [0.00]	-0.17 [0.00]
***R*-ClusterI**	QPLD SP/SP	0.06 [0.04]	0.38 [0.03]	-0.42 [0.07]	0.19 [0.04]	-0.44 [0.02]	-0.19 [0.00]
	QPLD SP/XP	0.06 [0.04]	0.37 [0.04]	-0.44 [0.08]	0.20 [0.04]	-0.44 [0.02]	-0.19 [0.00]
	QPLD XP/XP	0.07 [0.09]	0.40 [0.02]	-0.42 [0.05]	0.19 [0.03]	-0.43 [0.01]	-0.19 [0.01]
***R*-ClusterII**	QPLD SP/SP	0.03 [0.06]	0.36 [0.02]	-0.41 [0.06]	0.21 [0.05]	-0.45 [0.02]	-0.18 [0.01]
	QPLD SP/XP	0.01 [0.06]	0.36 [0.02]	-0.36 [0.18]	0.21 [0.05]	-0.45 [0.02]	-0.18 [0.01]
	QPLD XP/XP	-0.02 [0.00]	0.37 [0.00]	-0.38 [0.03]	0.19 [0.03]	-0.42 [0.00]	-0.19 [0.00]

Grid calculations - Prior to Grid calculations the binding sites of the involved protein-ligand complexes were minimized with MacroModel[46] in the gas phase by Conjugated Gradient method with the OPLS-AA[27] force field. The ligand was chosen to define the center and a shell of 8 Å around the center was allowed to move freely during the minimization. Furthermore, surrounding the freely moving area, a shell of 10 Å was applied with a force constant of 200 kJ/molÅ^2 allowing only moderate flexibility of the protein structure. The rest of the protein was frozen during the calculation.

The binding sites of the different binding modes were characterized by molecular interaction fields (MIFs), calculated in the GRID v22a software.[47] Hydrogen atoms and the bound ligands were deleted from the minimized protein-ligand complexes. Furthermore, the atom types of the ions and residue names of Glu508 and Asp524 were corrected according to the grub.dat file in the GRID program. The probes used were C3 (CH_3 methyl group), N1+ (sp^3-hybridized amine-NH cation), N:# (sp-hybridized nitrogen atom with a lone pair), OFU (furan oxygen atom), and F (organic fluorine atom). The box dimensions were defined to assure all relevant residues lining the binding site were included. This resulted in a box size of 20Å x 20Å x 20 Å. The Grid spacing was set to 0.25 Å, and the number of extra target atoms were set to three to make sure the ions in the model were considered in the calculations.

Docking in extracellular vestibular S2-site. Table S4 outlines the performed IFD dockings of *R*- and *S*-citalopram into the vestibular S2-site of hSERT. The IFD protocol was applied with the XP-scoring function in the final re-docking stage. A maximum of 100 poses were returned for each simulation.

Table S4. Statistics of the IFD dockings into the S2-site. Only poses placing the flouro-group in the proposed halogen binding pocket (HBP) are included in the statistics below.

Ligand in central cavity	**Ligand docked into S2 site**	**Number of poses in HBP**	**Average G-score**	**N^+ interacts with**
5-HT	*R*-**1**	2/4	-9.3 [0.7]	Glu493
***R*-ClusterI**	*R*-**1**	N/A	N/A	N/A
***R*-ClusterII**	*R*-**1**	N/A	N/A	N/A
***S*-ClusterI**	*R*-**1**	1/6	-7,1	Gly402
***S*-ClusterII**	*R*-**1**	0	N/A	N/A
5-HT	*S*-**1**	1/3	-7.5	Gly402
***R*-ClusterI**	*S*-**1**	6/29	-9.5 [0.7]	Tyr107 (cation···π) Ala401
***R*-ClusterII**	*S*-**1**	1/2	-7.1	Asp98
***S*-clusterI**	*S*-**1**	2/7	-8.2 [2.0]	Ala401, Gly402
***S*-ClusterII**	*S*-**1**	1/8	-11.0	Ala401

Synthesis of citalopram-analogs

Synthesis of citalopram analogs was carried out from either homochiral citalopram (*S*-**1**, *R*-**1**) or from achiral starting materials involving chiral SFC (supercritical fluid chromatography) product separation.

Compounds *R*-**6**, *S*-**6**, *R*-**7**, and *S*-**7** were all prepared from homochiral citalopram (escitalopram (*S*-**1**) or R-citalopram (*R*-**1**), Scheme 1). The nitrile group underwent hydrolysis under alkaline conditions followed by Fischer esterification in the presence of triethylorthoformate to give *R*-**6** and *S*-**6** in 94% yield over two steps. To attain *R*-**7** and *S*-**7**, the ester function of *R*-**6** and *S*-**6**, respectively, were reduced by lithium aluminum hydride in 90% yield.

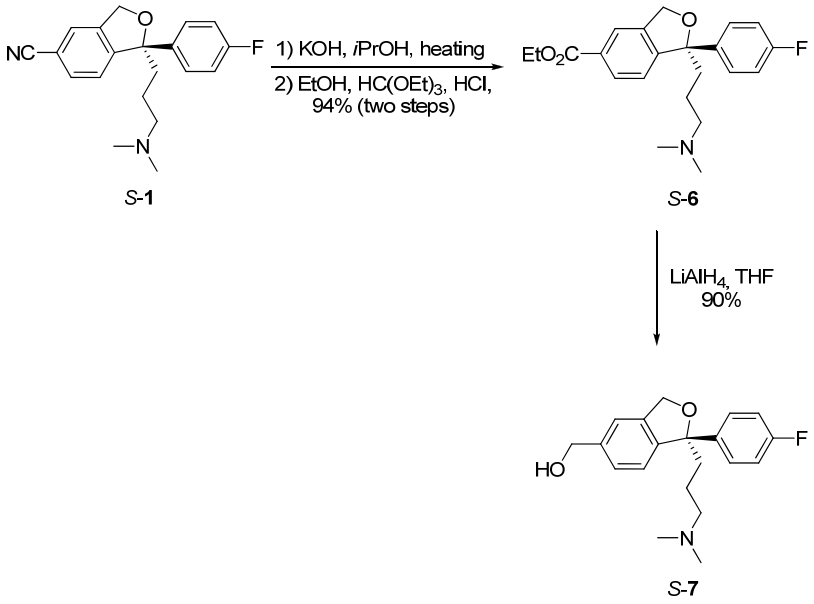

Scheme 1. Synthesis of *S*-6/*R*-6 and *S*-7/*R*-7 from homochiral *S*-1/*R*-1 exemplified as described for *S*-1.

The synthesis of *R*-**4**/*S*-**4** was carried out from achiral phthalide **8** (Scheme 2). Addition of first aryl Grignard reagent A and then alkyl Grignard B in a one-pot procedure gave diol (±)-**9** in 39%. Methanesulfonyl chloride mediated cyclisation gave (±)-**4** in a moderate yield (45%). The racemate ((±)-**4)** was separated by SFC to give each enantiomer *R*-**4** and *S*-**4** in 97.9% and 99.0% enantiomeric excess (ee), respectively.

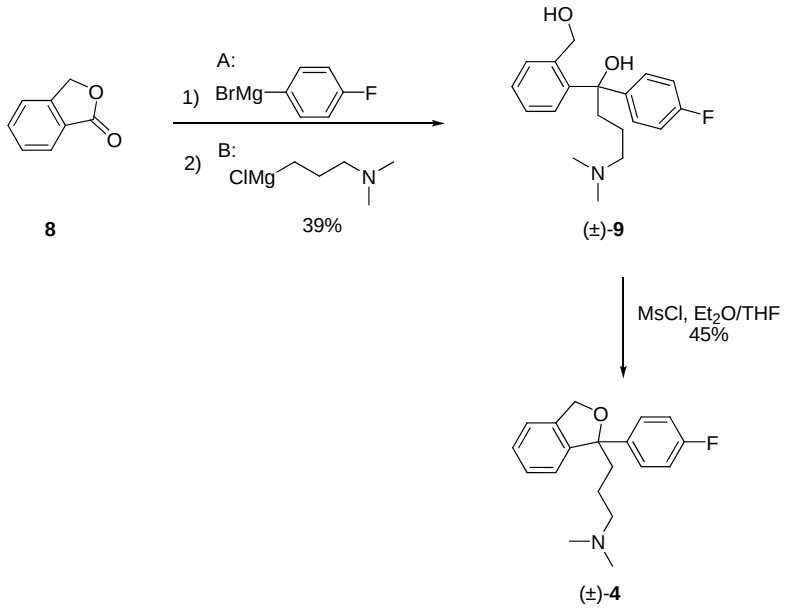

Scheme 2. Synthesis of racemic (±)-4 from phthalide 8.

To establish absolute configuration, bromo-escitalopram *S*-**10** was dehalogenated by first reaction with *n*BuLi followed by protonation (Scheme 3). By chiral HPLC analysis the product (*S*-isomer) was found to correlate with the slow isomer ascertaining this as *S*-**4**.

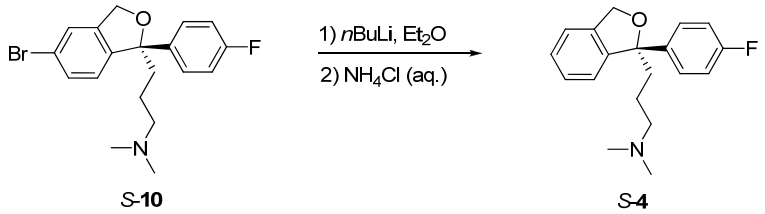

Scheme 3. Synthesis of *S*-4 by dehalogenation to establish absolute configuration.

Hydroxymethyl substituted citaloprams *R*-**5** and *S*-**5** were prepared by reacting cyanophthalide **11** with first Grignard reagent C and then Grignard reagent B in a procedure similar to the synthesis of (±)-**4** (Scheme 4). The diol (±)-**12** was obtained in 60% yield and subsequently cyclized to give (±)-**13** in excellent yield (95%). The tetrahydropyridyl (THP) protecting group was removed by treatment with *p*-TsOH in methanol to give the free primary alcohol (±)-**5** in 80% yield. The racemate was separated into enantiomers, fractions being 99.4% and 97.6% ee by SFC.

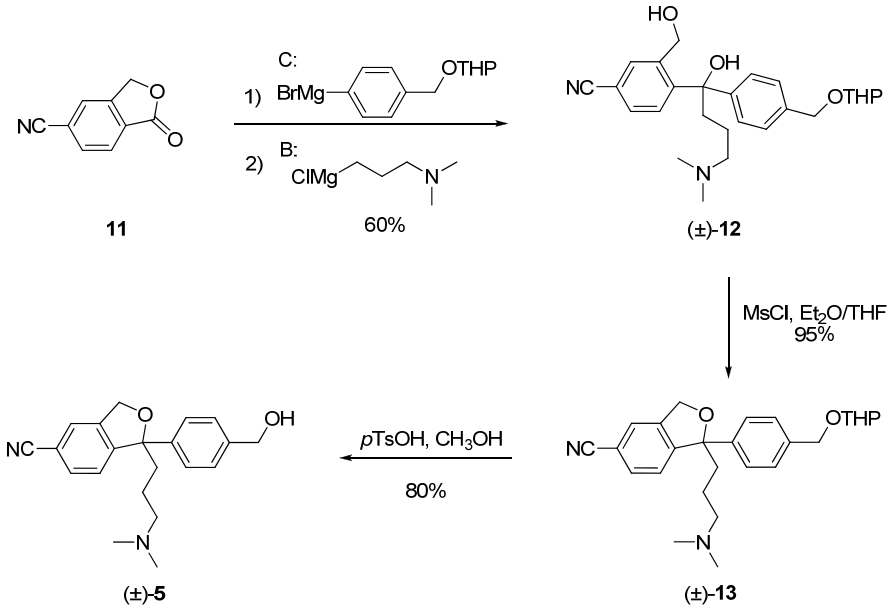

Scheme 4. Synthesis of racemic (±)-5 from cyanophthalide 11.

The evidence for establishing (+)-**5** as *S*-**5** and (-)-**5** as *R*-**5** is circumstantial, but nevertheless overwhelmingly probable. The *S*-isomers were found consequently to be dextrorotatory and have the highest inhibitory potential. It was not possible to extrapolate any useful information from HPLC and SFC retention times since no single column used was able to separate all sets of enantiomers.

Table S5. Overview of physical data for citalopram and analogs. [a](c 1, CH_2Cl_2), *(c 1, CH_3OH); [b]R_t (retention time) in heptane/EtOH/Et_2NH on chiral HPLC (ODH column), [c]R_t in heptane/EtOH/Et_2NH (ADH column), [d]R_t in hexan/EtOH/Et_2NH/propionic acid (ADH column), [e]K_i-values for 5-HT uptake against wtSERT, [f]R_t in MeOH/Et_2NH (ADH column), [g]R_t in EtOH/Et_2NH (ASH column), [h]R_t in EtOH/Et_2NH (LUX01 column).

Compound	$[\alpha]_D$[a]	HPLC: R_t (min)	SFC: R_t (min)	K_i[e] (nM)
S-**1**	+4.7	25.5[b]	3.50	9.2
R-**1**	-5.5	23.0[b]	2.79	370
S-**4**	+1.4	14.9[c]	4.15[f]	54
R-**4**	-2.0	13.9[c]	5.11[f]	730
(+)-**5**	+4.5	22.7[d]	2.39[g]	83
(-)-**5**	-5.0	19.0[d]	2.78[g]	1050
S-**6**	+4.0	11.7[b]	3.21[h]	86
R-**6**	-7.0	8.3[b]	4.40[h]	1930
S-**7**	+5.0*	57.1[b], 10.1[d]	4.60[h]	60
R-**7**	-4.0*	82.2,[b] 11.2[d]	4.41[h]	590

General Experimental Information:

Reaction and solvents: All reagents except otherwise stated were used as purchased without further purification. Dried glassware from the oven (ca. 120 °C) was used for reactions carried out under nitrogen or argon atmosphere. Solvents were dried according to standard procedures prior to use ('Purification of Laboratory Chemicals, 3rd Edition' D. D. Perrin, W. L. F. Armarego, 1988, Butterworth-Heinemann Ltd). Dichloromethane was dried by distillation over CaH_2, and diethyl ether was dried over sodium. THF was dried over sodium and distilled with benzophenone.

'Bromo-escitalopram' (**10**), *S*-Citalopram (*S*-**1**), *S*-demethylcitalopram (*S*-**2**), *S*-didemethylcitalopram (*S*-**3**), and antipodes thereof (*R*-**1**, *R*-**2**) were kindly donated by H. Lundbeck A/S.

Chromatography: Flash chromatography was performed with Merck silica 60 (230-400 mesh) as stationary phase. TLC was performed on silica-coated glass plates (Merck 60 F_{254}). TLC plates were first observed in UV-light and then visualized with:

1) Anizaldehyde-stain (3.7 mL p-anisaldehyde in 5 mL conc. H_2SO_4, 1.5 mL AcOH and 135 mL abs. EtOH)

2) $KMnO_4$-stain (1.5 g $KMnO_4$ in 1.25 mL 10% NaOH and 200 mL H_2O)

Apparatus: ^{1}H-NMR (400 MHz) and ^{13}C-NMR (100 MHz) were recorded at a Varian Mercury 400 spectrometer. $CDCl_3$ (δ 7.26 ppm ($CHCl_3$) for proton and δ 77.16 ppm for carbon resonances) and DMSO (δ 2.50 ppm for proton and 39.52 for carbon resonances) were used as internal references. NMR spectral assignments are based on *g*COSY, *g*HMQC, and DEPT-135 experiments. MS spectra were recorded at a Micromass LC-TOF instrument by using electrospray ionization (ESI). High resolution spectra were recorded with either of the following compounds as internal standard: (Boc-L-alanine: $C_8H_{15}NO_4Na$: 212.0899; BzGlyPheOMe: $C_{19}H_{20}N_2O_4Na$: 363.3629; BocSer(OBn)SerLeuOMe: $C_{25}H_{39}N_3O_8Na$: 532.2635; erythromycin: $C_{37}H_{67}NO_{13}Na$: 756.4510) Masses of standards and analytes are calculated and reported in Daltons for un-charged species.

Melting points were measured on a Büchi B-540 instrument and are uncorrected. Optical rotation was measured on a PE-314 polarimeter and reported in units of deg*cm^2/g. Concentrations are reported in g/100 mL.

General procedure for preparation of Grignard reagents (A, B, C).

An alkyl or aryl halide (1 eq.) was added dropwise to Mg (1.5 eq.) in dry THF under N_2 atm. at such a rate that the solution was kept at gentle reflux. After the addition was completed, the mixture was heated to reflux for an additional 1-3 hours. Before being taken out via a syringe and used in the reaction, the Grignard reagent was titrated according to a known procedure.[48]

Ethyl 1-(3-Dimethylaminopropyl)-1-(4-fluorophenyl)-1,3-dihydroisobenzofuran-5-carboxylate, *S*-6 and *R*-6:

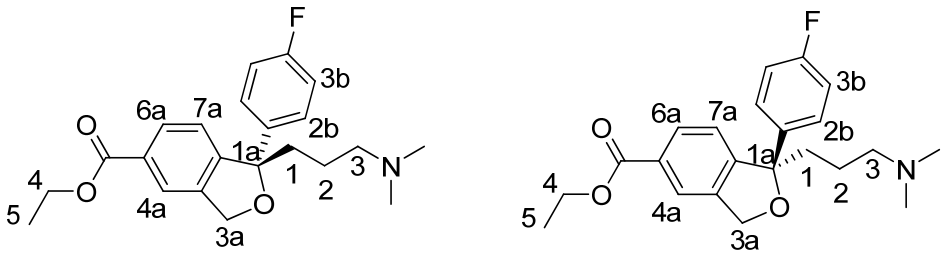

Identical procedure for both enantiomers:

Escitalopram oxalate (*S*-**1**, 332 mg, 0.8 mmol) was dissolved in a 5M solution of KOH in isopropanol (25 mL) and heated to 100 °C overnight. The reaction mixture was cooled to ambient temperature and acidified to pH~2 by addition of 6M hydrochloric acid before evaporated to dryness under reduced pressure. The remaining solid was then dissolved in absolute ethanol (40 mL) and triethylorthoformate (10 mL) and cooled to 0 °C before acetylchloride (4 mL) slowly was added. The reaction mixture was refluxed overnight, cooled to ambient temperature, poured into saturated $NaHCO_3$ (aq.) and extracted with CH_2Cl_2 (3*50 mL), dried over $MgSO_4$ and concentrated under reduced pressure to afford the crude ester. This was taken up in ether (30 mL) and extracted with hydrochloric acid (6M, 2*20 mL). The combined aqueous extracts was neutralized by careful addition of solid $NaHCO_3$ and extracted with CH_2Cl_2 (2*20 mL). The combined organic extracts were dried over $MgSO_4$, filtered and concentrated under reduced pressure to give ethyl ester (277 mg, 94%) as a colorless oil. R_f (AcOEt/Et_3N 1:0.05) 0.32. ^{1}H-NMR ($CDCl_3$, 400 MHz) δ_H 7.98 (d, 1H, $J_{6a,7a}$ 8 Hz, H6a/H7a), 7.88 (s, 1H, H4a), 7.44 (dd, 2H, $J_{o,H\text{-}H}$ 8 Hz, $J_{m,H\text{-}F}$ 5.6 Hz, H2b), 7.33 (d, 1H, $J_{6a,7a}$ 8 HZ, H7a/H6a), 6.98 (t, 2H, $J_{o,H\text{-}H/H\text{-}F}$ 8.8 Hz, H3b), 5.19 (d, J_{gem} 12.6 Hz, H3a), 5.14 (d, J_{gem} 12.6 Hz, H3a'), 4.36 (q, 2H, $J_{4,5}$ 7.2 Hz, H4), 2.25 (t, 2H, $J_{2,3}$ 7.2 Hz, H3), 2.21-2.11 (m, 2H, H1), 2.14 (m, 6H, N(CH_3)$_2$), 1.52-1.45 (m, 1H, H2), 1.37 (t, 3H, $J_{4,5}$ 7.2 Hz, H5), 1.39-1.27 (m, 1H, H2). ^{13}C-NMR ($CDCl_3$, 100 MHz) δ_C 166.3 (CO), 162.0 ($J_{C\text{-}F}$ 244 Hz, C4b), 149.1 (Ar), 140.4 ($J_{C\text{-}F}$ 3.1 Hz, C1b), 139.6, 130.4, 129.4 (Ar), 127.0 ($J_{C\text{-}F}$ 8.4 Hz, C2b), 122.7, 121.9 (Ar), 115.2 ($J_{C\text{-}F}$ 20.6 Hz, C3b), 91.0 (C1a), 71.7 (C3a), 61.2 (C4), 59.6 (C3), 45.4 (N(CH_3)$_2$), 39.2 (C1), 22.2 (C2), 14.4 (C5). HRMS(ES): calcd. for $C_{22}H_{27}FNO_3$ 372.1975. found: 372.1976. $[\alpha]_D^{20}$ (*S*-**6**) + 4 (*c* 1, CH_2Cl_2). $[\alpha]_D^{20}$ (*R*-**6**) - 7 (*c* 1, CH_2Cl_2).

_S_-1-(3-Dimethylaminopropyl)-1-(4-fluorophenyl)-5-hydroxymethyl-1,3-dihydroisobenzofuran and _R_-1-(3-Dimethylaminopropyl)-1-(4-fluorophenyl)-5-hydroxymethyl-1,3-dihydroisobenzofuran, _S_-7 and _R_-7:

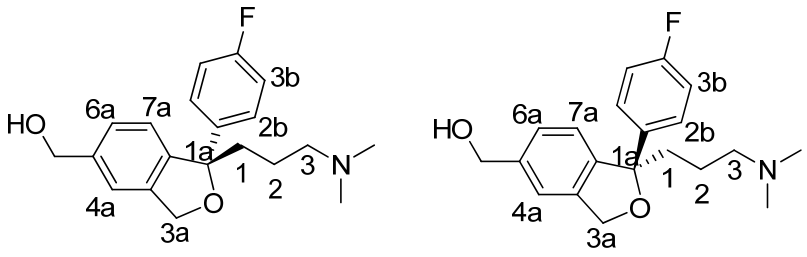

Identical procedure for both enantiomers:

Ethyl ester (*R*-**6**) (305 mg, 0.82 mmol) was dissolved in dry THF (10 mL) and cooled to 0 °C, whereupon $LiAlH_4$ (130 mg, 3.4 mmol) was added. The reaction mixture was stirred at room temperature for 3.5 hours. An aqueous saturated solution of potassium-sodium tartrate (10 mL) was added, and the mixture was stirred at room temperature for 30 min. The mixture was then extracted with CH_2Cl_2 (3*20 mL), the combined organic phases dried over $MgSO_4$ and concentrated under reduced pressure. Purification was accomplished using flash chromatography (AcOEt → AcOEt/Et_3N 1:0.05) to afford the desired alcohol (*R*-**7**) (245 mg, 90 %) as a colorless oil. R_f (CH_2Cl_2/CH_3OH/Et_3N 95/2.5/2.5) 0.43.

^{1}H-NMR ($CDCl_3$, 400 MHz) δ_H 7.50 (dd, 2H, J_o 8.2 Hz, $J_{m,H\text{-}F}$ 5.2 Hz, H2b), 7.31 (s, 3H, H4a, H6a, H7a), 7.02 (t, 2H, $J_{o,H\text{-}H/H\text{-}F}$ 8.2 Hz, H3b), 5.20 (d, 1H, J_{gem} 12.6 Hz, H3a), 5.16 (d, 1H, J_{gem} 12.6 Hz, H3a), 4.71 (s, 1H, O*H*), 2.31 (t, 2H, $J_{2,3}$ 7.4 Hz, H3), 2.20 (s, 6H, $N(CH_3)_2$), 2.13-2.28 (m, 2H, H1), 1.59-1.49 (m, 1H, H2), 1.45-1.33 (m, 1H, H2). ^{13}C-NMR ($CDCl_3$, 100 MHz) δ_C 162.8 ($J_{C\text{-}F}$ 243 Hz, C4b), 143.4, 141.3 (Ar), 141.2 ($J_{C\text{-}F}$ 3.1 Hz, C1b), 139.5 (Ar), 126.9 ($J_{C\text{-}F}$ 8.4 Hz, C2b), 126.4, 121.9, 119.8, (Ar), 115.0 ($J_{C\text{-}F}$ 20.7 Hz, C3b), 90.9 (C1a), 71.9 (C3a), 64.6 (CH_2OH), 59.7 (C3), 45.3 ($N(CH_3)_2$), 39.4 (C1), 22.2 (C2). HRMS(ES): calcd. for $C_{20}H_{25}FNO_2$ 330.1869; found 330.1874. $[\alpha]_D^{20}$ (*S*-**7**) + 5 (*c* 1, CH_3OH).

$[\alpha]_D^{20}$ (*R*-**7**) - 4 (*c* 1, CH_3OH).

2-(4-bromobenzyloxy)tetrahydro-*2H*-pyran.

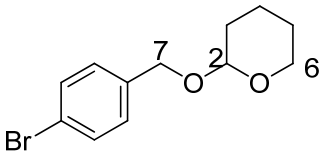

A solution of 4-bromobenzyl alcohol (5.011 g, 26.8 mmol), DHP (2.7 mL, 29.6 mmol) and $TsOH{\cdot}H_2O$ (5 mg, cat.) in CH_2Cl_2 (20 mL) was stirred at room temperature for 2 hours. The solution was poured into saturated aqueous $NaHCO_3$ and extracted thrice times with CH_2Cl_2, dried over Na_2SO_4 and concentrated under reduced pressure. The product was purified by flash chromatography (AcOEt/petrol 1:15) to give the desired THP-protected alcohol (6.449 g, 89%) as a yellow oil. R_f (AcOEt/petrol 1:15) 0.30. ^{1}H-NMR ($CDCl_3$, 400 MHz) δ_H 7.46 (d, 2H, J_o 8.4 Hz, Ar*H*), 7.24 (d, 2H, J_o 8.4 Hz, Ar*H*), 4.73 (d, 1H, J_{gem} 12.4 Hz, H7), 4.69 (t, 1H, $J_{2,3}$ 3.6 Hz, H2), 4.45 (d, 1H, J_{gem} 12.4 Hz, H7'), 3.86-3.93 (m, 1H, H6eq), 3.59-3.51 (m, 1H, H6ax), 1.90-1.80 (m, 1H, THP), 1.79-1.70 (m, 1H, THP), 1.69-1.51 (m, 4H, THP). Data was in accordance with ref. [49]

^{13}C-NMR ($CDCl_3$, 100 MHz) δ_C 137.5, 131.6, 129.5, 121.5 (Ar), 98.0 (C2), 68.2 (C7), 62.3 (C6), 30.6 (C3), 25.6 (C5), 19.4 (C4). LRMS(ES): calcd. for $C_{12}H_{15}O_2{}^{79}BrNa$: 293.0; found 293.0.

(±) 4-[4-(Dimethylamino)-1-hydroxy-1-(4-((tetrahydro-*2H*-pyran-2-yloxy)methyl) phenyl)butyl)-3-(hydroxymethyl)benzonitrile, 12.

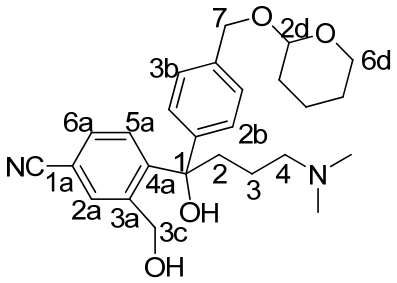

A 1 M solution of the THP-protected Grignard reagent C (Scheme 4) in dry THF (8.88 mL, 8.88 mmol) was prepared as described above. This was added to 5-cyanophthalide (**11**) (1.180 g, 7.4 mmol) in dry THF (10 mL) at 0 °C under N_2 atmosphere. The reaction mixture was stirred at room temperature overnight. A 1.6 M solution of the Grignard reagent B in dry THF (7.5 mL, 12 mmol) was prepared from 3-chloro-1-*N*,*N*-dimethyl-propylamine and added to the reaction mixture. The mixture was stirred at room temperature overnight, whereupon it was quenched with CH_3OH, concentrated under reduced pressure and purified by flash chromatography (AcOEt/petrol 1:1 → AcOEt/Et_3N 1:0.03) to afford the product as yellow oil (1.94 g, 60%). R_f (AcOEt/Et_3N 1:0.03) 0.25. ^{1}H-NMR ($CDCl_3$, 400 MHz) δ_H 7.59-7.53 (m, 3H, Ar), 7.27-7.22 (m, 4H, Ar), 4.70 (d, 1H, J_{gem} 11.8 Hz, H7), 4.64 (m, 1H, H2d), 4.42 (d, 1H, J_{gem} 12.6 Hz, H3c), 4.40 (d, 1H, J_{gem} 11.8 Hz, H7'), 4.09 (d, 1H, J_{gem} 12.6 Hz, H3c'), 3.87-3.81 (m, 1H, H6eq), 3.52-3.45 (m, 1H, H6ax), 2.42-2.37 (m, 2H, H4), 2.34-2.28 (m, 2H, H3), 2.17 (s, 6H, $N(CH_3)_2$), 1.84-1.74 (m, 1H, H2), 1.72-1.64 (m, 1H, H2'), 1.63-1.45 (m, 6H, THP). ^{13}C-NMR ($CDCl_3$, 100 MHz) δ_C 151.2, 146.0, 142.2, 136.7, 135.2, 130.6, 127.3, 125.9, 118.5 (Ar), 111.0 (CN), 97.9 (C2d), 77.6 (C1), 68.4 (C7), 63.8 (C3c), 62.1 (C6d), 59.9 (C4), 44.7 ($N(CH_3)_2$), 43.6 (C2), 30.5 (C3d), 25.4 (C5d), 22.1 (C3), 19.3 (C4d). HRMS(ES): calcd. for $C_{26}H_{34}N_2O_4Na$ 461.2416; found 461.2433.

(±)1-(3-Dimethylaminopropyl)-1-(4-((tetrahydro-*2H*-pyran-2-yloxy)methyl)phenyl)-1,3-dihydroisobenzofuran-5-carbonitrile, 13.

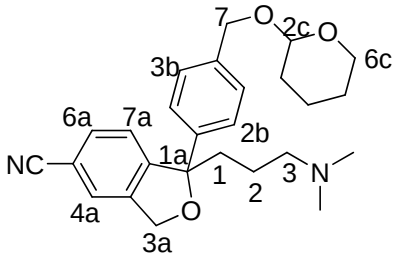

To a solution of diol **12** (276 mg, 0.63 mmol) in dry ether (10 mL) and dry THF (3 mL) was added Et_3N (0.26 mL, 1.87 mmol), then MsCl (0.06 mL, 0.77 mmol) at 0 °C. The reaction mixture was stirred at 0 °C for 30 min. before poured into saturated aqueous $NaHCO_3$ (20 mL) and extracted with ether (3*20 mL). The combined organic layers were dried over Na_2SO_4, filtered, and concentrated under reduced pressure to afford the product as yellow oil (253 mg, 95 %). Further purification was not necessary. R_f (AcOEt/Et_3N 1:0.03) 0.29.

^{1}H-NMR ($CDCl_3$, 400 MHz) δ_H 7.57 (d, 1H, J_o 7.6 Hz, H6a/H7a), 7.48 (s, 1H, H4a), 7.43 (d, 2H, J_o 8.0 Hz, H2b), 7.42 (d, 1H, J_o 7.6 Hz, H7a/H6a), 7.32 (d, 2H, J_o 8.0 Hz, H3b), 5.20 (d, 1H, J_{gem} 12.8 Hz, H3a), 5.15 (d, 1H, J_{gem} 12.8 Hz, H3a'), 4.74 (d, 1H, J_{gem} 12 Hz, H7), 4.67 (t, 1H, $J_{2d,3d}$ 3.6 Hz, H2c), 4.44 (d, 1H, J_{gem} 12 Hz, H7'), 3.92-3.86 (m, 1H, H6eq), 3.56-3.56 (m, 1H, H6ax), 2.30 (t, 2H, $J_{2,3}$ 7.4 Hz, H3), 2.19 (s, 6H, $N(CH_3)_2$), 2.26-2.26 (m, 2H, H1), 1.88-1.79 (m, 1H, H2), 1.76-1.68 (m, 1H, H2'), 1.65-1.31 (m, 6H, THP). ^{13}C-NMR ($CDCl_3$, 100 MHz) δ_C 149.5, 142.8, 140.2, 137.4, 131.6, 127.9, 125.0, 124.9, 122.7, 118.6 (Ar), 111.4 (CN), 97.7 (C2c), 91.2 (C1a), 71.2 (C3a), 68.3 (C7), 62.0 (C6c), 59.3 (C3), 45.1 ($N(CH_3)_2$), 38.7 (C1), 30.4 (C3c), 25.3 (C5c), 21.8 (C2), 19.2 (C4c). HRMS(ES): calcd. for $C_{26}H_{33}N_2O_3$ 421.2491; found 421.2505.

(±)1-(3-Dimethylaminopropyl)-1-(4-(hydroxymethyl)phenyl)-1,3-dihydroisobenzofuran-5-carbonitrile, (±)-5.

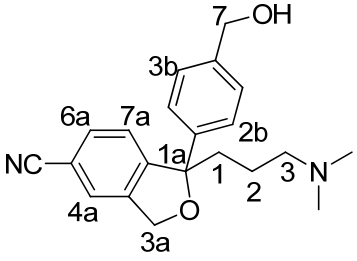

A solution of **13** (304 mg, 0.72 mmol) and *p*-TsOH·H_2O (146 mg, 0.77 mmol) in CH_3OH (7 mL) was stirred at room temperature for 2 hours. The solution was quenched by addition of an aqueous saturated solution of $NaHCO_3$ (10 mL). CH_3OH was removed under reduced pressure, and the aqueous solution extracted with CH_2Cl_2 (3*10 mL). The combined organic extracts were dried over Na_2SO_4 and concentrated under reduced pressure. Purification was accomplished using flash chromatography (AcOEt → AcOEt/Et_3N 1:0.03) to afford the product as yellow oil (195 mg, 80 %). R_f (AcOEt/CH_3OH/Et_3N 1:0.025:0.03) 0.23. ^{1}H-NMR ($CDCl_3$, 400 MHz) δ_H 7.57 (d, 1H, J_o 8.0 Hz, H6a/H7a), 7.48 (s, 1H, H4a), 7.45 (d, 2H, J_o 8.2 Hz, H2b), 7.43 (d, 1H, J_o 8.0 Hz, H7a/H6a), 7.32 (d, 2H, J_o 8.2 Hz, H3b), 5.21 (d, 1H, J_{gem} 13.2 Hz, H3a), 5.16 (d, 1H, J_{gem} 13.2 Hz, H3a'), 4.65 (s, 2H, H7), 2.26-2.22 (m, 2H, H3), 2.14 (s, 6H, $N(CH_3)_2$), 2.22-2.11 (m, 2H, H1), 1.50-1.42 (m, 1H, H2), 1.38-1.31 (m, 1H, H2'). ^{13}C-NMR ($CDCl_3$, 100 MHz) δ_C 149.6, 142.6, 140.7, 140.2, 131.9, 127.2, 125.2, 125.1, 122.9, 118.7 (Ar), 111.6 (CN), 91.3 (C1a), 71.4 (C3a), 64.3 (C7), 59.1 (C3), 44.7 ($N(CH_3)_2$), 38.6 (C1), 21.5 (C2). HRMS(ES): calcd. $C_{21}H_{25}N_2O_2$ for 337.1916; found 337.1906.

(*S*)-1-(3-Dimethylaminopropyl)-1-(4-(hydroxymethyl)phenyl)-1,3-dihydroisobenzofuran-5-carbonitrile, (*S*-5) and (*R*)-1-(3-Dimethylaminopropyl)-1-(4-(hydroxymethyl)phenyl)-1,3-dihydroisobenzofuran-5-carbonitrile, (*R*-5).

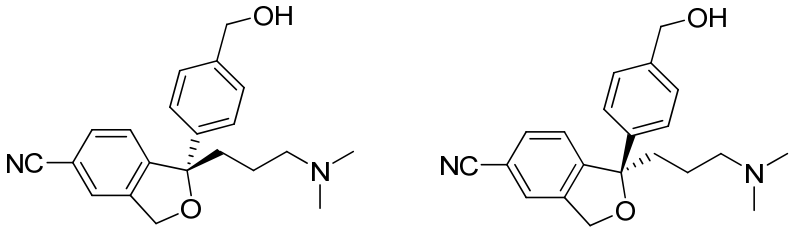

Racemic **5** ((±)-**5**) were separated to their two enantiomers by preparative SFC:

Column: AS-H, 4.6x250 mm, 5 μM

Modifier: EtOH + 0.1 % DEA

Modifier conc.: 15 %

Flow: 4 mL/min.

UV: 230 nm

Temp.: 40°C

Pressure: 200 bar

Injection volume: 15 µL

Fraction 1: ee 99.4 %

Fraction 2: ee 97.6 %.

$[\alpha]_D^{20}$ (*S*-**5**, fraction 1) + 4.5 (*c* 1, CH_2Cl_2).

$[\alpha]_D^{20}$ (*R*-**5**, fraction 2) - 5 (*c* 1, CH_2Cl_2).

(±)-4-(Dimethylamino)-1-(4-fluorophenyl)-1-(2-(hydroxymethyl)phenyl)butan-1-ol, 9.

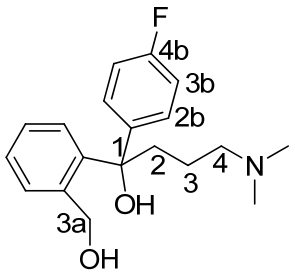

A 1 M solution of the Grignard reagent A (Scheme 2) in dry THF (8.9 mL, 8.9 mmol) was made as described above and added to phthalide (**8**) (1.0 g, 7.5 mmol) in THF (10 mL) at 0 °C under an atmosphere of N_2. The mixture was stirred at room temperature overnight before a 1.6 M solution of the Grignard reagent B (Scheme 2) in THF (7.5 mL, 12 mmol) was added to this mixture, which was then stirred at reflux overnight. The mixture was quenched with ice water, basified with aqueous ammonia (25% by weight), extracted with CH_2Cl_2 (4*50 mL), dried over $MgSO_4$ and concentrated under reduced pressure. The product was purified by flash chromatography (AcOEt → AcOEt/Et_3N 1:0.03) to give the desired diol (937 mg, 39 %) as a yellow oil. R_f (AcOEt/Et_3N 1:0.03) 0.26. ^{1}H-NMR ($CDCl_3$, 400 MHz) δ_H 7.47 (d, 1H, J_o 8.0 Hz, ArH), 7.26-7.35 (m, 5H, ArH), 6.94 (t, 2H, $J_{o,H\text{-}H/H\text{-}F}$ 8.8 Hz, H3b), 4.37 (d, 1H, J_{gem} 11.6 Hz, H3a), 4.13 (d, 1H, J_{gem} 11.6 Hz, H3a'), 2.56-2.48 (m, 1H, H4), 2.42-2.32 (m, 3H, H2, H4), 2.23 (s, 6H, $N(CH_3)_2$), 1.77-1.67 (m, 1H, H3), 1.59-1.51 (m, 1H, H3'). ^{13}C-NMR ($CDCl_3$, 100 MHz) δ_C 161.3 ($^1J_{C\text{-}F}$ 243 Hz, C4b), 145.8 (Ar), 144.1 ($^4J_{C\text{-}F}$ 3 Hz, C1b), 140.6, 132.7 (Ar), 127.7 ($^3J_{C\text{-}F}$ 8.4 Hz, C2b), 127.6, 127.1, 126.4 (Ar), 114.4 ($^2J_{C\text{-}F}$ 20.6 Hz, C3b), 77.6 (C1), 64.8 (C3a), 60.0 (C4), 44.8 ($N(CH_3)_2$), 43.9 (C2), 22.3 (C3). HRMS (ES): calcd. for $C_{19}H_{24}FNO_2Na$ 340.1689; found 340.1690.

(±)-3-(1-(4-fluorophenyl)-1,3-dihydroisobenzofuran-1-yl)propyl-dimethylamine, 4.

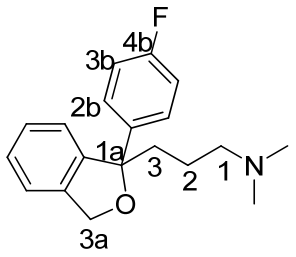

To a stirred solution of diol **9** (475 mg, 1.5 mmol) in dry ether (15 mL) and dry THF (10 mL) was added Et_3N (0.6 mL, 4.3 mmol), then MsCl (0.14 mL, 1.8 mmol) at 0 °C. The reaction mixture was stirred at 0 °C for 30 min., poured into saturated aqueous $NaHCO_3$ (20 mL), extracted with ether (3*20 mL), dried over Na_2SO_4, filtered and concentrated under reduced pressure. Purification was accomplished using flash chromatography (AcOEt/petrol/Et_3N 2:1:0.03 $\rightarrow$ 1:0:0.03) to afford the desired product as a yellow oil (200 mg, 45%). R_f (AcOEt/Et_3N 1:0.03) 0.35. ^{1}H-NMR ($CDCl_3$, 400 MHz) δ_H 7.48-7.43 (m, 2H, ArH), 7.29-7.27 (m, 2H, ArH), 7.26-7.22 (m, 1H, ArH), 7.21-7.18 (m, 1H, ArH), 7.01-6.94 (m, 2H, ArH), 5.17 (d, 1H, J_{gem} 12.2 Hz, H3a), 5.13 (d, 1H, J_{gem} 12.2 Hz, H3a'), 2.23 (m, 2H, H1), 2.13 (s, 6H, $N(CH_3)_2$), 2.20-2.09 (m, 2H, H3), 1.53-1.42 (m, 1H, H2), 1.39-1.28 (m, 1H, H2'). ^{13}C-NMR ($CDCl_3$, 100 MHz) δ_C 161.9 ($^1J_{C\text{-}F}$ 244 Hz, C4b), 144.2 (Ar), 141.3 ($^4J_{C\text{-}F}$ 2.8 Hz, C1b), 139.1, 127.7, 127.6 (Ar), 127.0 ($^3J_{C\text{-}F}$ 7.6 Hz, C2b), 121.2, 122.0 (Ar), 115.0 ($^2J_{C\text{-}F}$ 21.4 Hz, C3b), 91.1 (C1a), 72.0 (C3a), 59.8 (C1), 45.5 ($N(CH_3)_2$), 39.5 (C3), 22.4 (C2). HRMS(ES): calculated for $C_{19}H_{22}OFNNa$ 322.1583; found 322.1534.

(*R*)-3-(1-(4-fluorophenyl)-1,3-dihydroisobenzofuran-1-yl)propyl-dimethylamine, *R*-4 and (*S*)-3-(1-(4-fluorophenyl)-1,3-dihydroisobenzofuran-1-yl)propyl-dimethylamine, *S*-4.

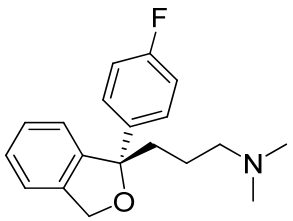

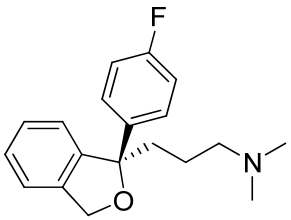

Racemic **4** ((±)-**4**) were separated to their two enantiomers by preparative SFC:

Column: AD-H, 4.6x250 mm, 5 µM

Modifier: MeOH + 0.2 % DEA

Modifier conc.: 8 %

Flow: 3 mL/min.

UV: 254 nm

Temp.: 40^{o}C

Pressure: 100 bar

Injection volume: 10 µL

Fraction 1: ee 99.0 %

Fraction 2: ee 97.9 %.

$[\alpha]_D^{20}$ (*S*-**4**, fraction1) + 1.4 (*c* 1, CH_2Cl_2)

$[\alpha]_D^{20}$ (*R*-**4**, fraction 2) - 2.0 (*c* 1, CH_2Cl_2).

(*S*)-3-(1-(4-fluorophenyl)-1,3-dihydroisobenzofuran-1-yl)propyl-dimethylamine, *S*-4 from (*S*)-(3-(5-bromo-1-(4-fluorophenyl)-1,3-dihydroisobenzofuran-1-yl)-propyl)-dimethylamine (bromo-escitalopram) *S*-10.

A stirred solution of bromo-escitalopram (500 mg, 1.32 mmol) and 2,2-dipyridyl (10 mg) in dry Et_2O (5 mL) under argon was cooled to −10 °C before *n*-BuLi (2 eq) was added slowly. The reaction mixture was stirred at this temperature for 2 hours before a saturated aqueous solution of NH_4Cl (10 mL) was added. The mixture was diluted with hydrochloric acid (0.1 M, 10 mL) and the aqueous layer washed with Et_2O (2*10 mL) before alkalized with a NaOH solution and extracted with CH_2Cl_2 (3*20 mL). Drying of the combined organic extracts over $MgSO_4$, filtration and concentration gave S-**4** (390 mg, crude). This was analyzed by chiral HPLC and compared to fractions obtained through the racemic synthetic route as described in Scheme 2.

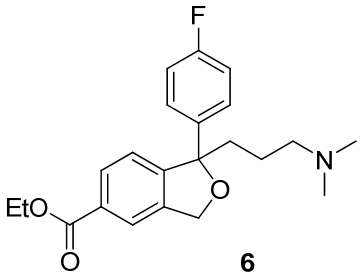
F
N
O
EtO
O

6

1.00
0.92
2.00
0.99
1.89
1.97
2.10
2.14
8.30
1.18
4.36
8.0
7.0
6.0
5.0
4.0
3.0
2.0
1.0
ppm (f1)

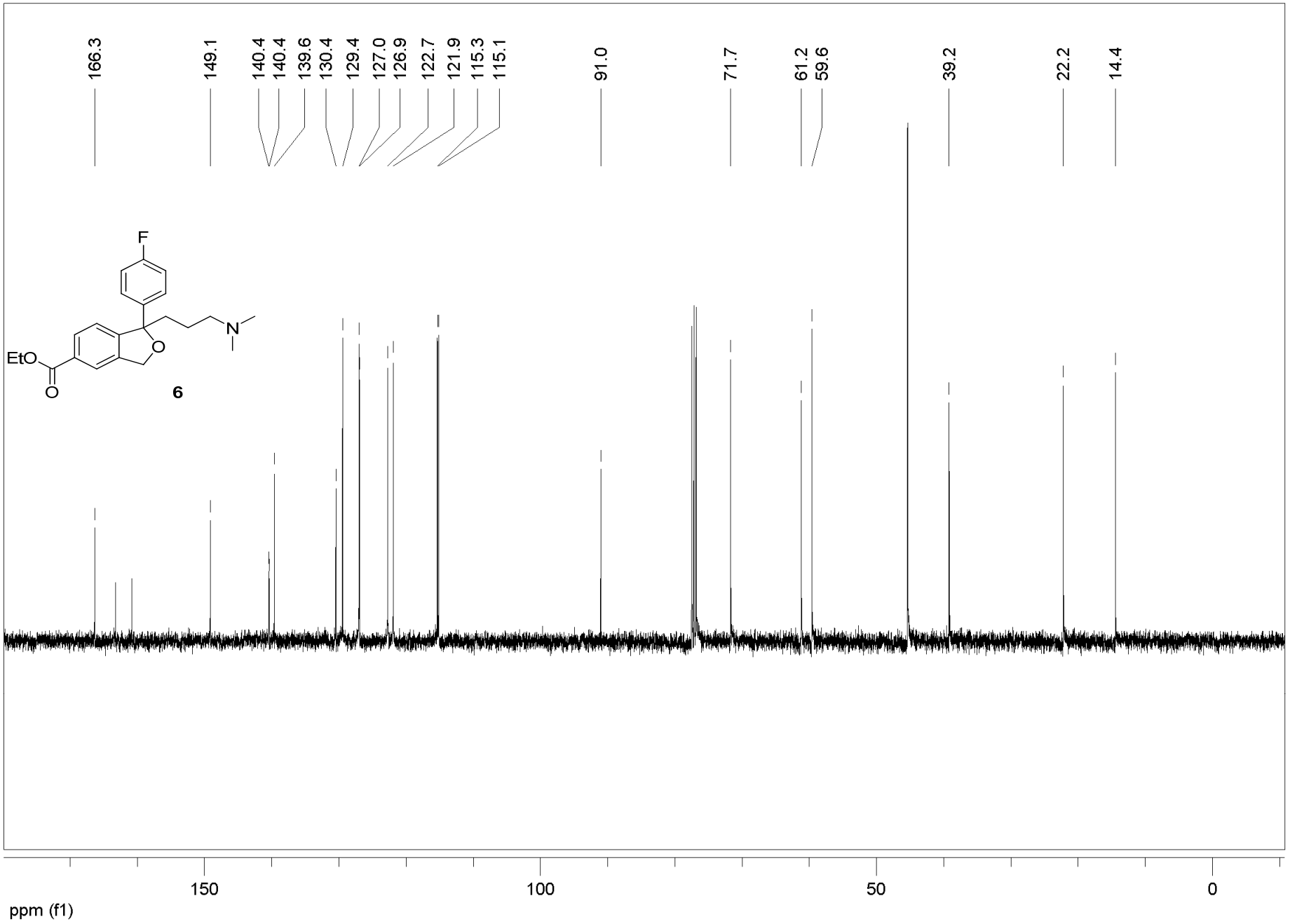
166.3
149.1
140.4
140.4
139.6
130.4
129.4
127.0
126.9
122.7
121.9
115.3
115.1
91.0
71.7
61.2
59.6
39.2
22.2
14.4
F
N
O
EtO
O
6
150
100
50
0
ppm (f1)

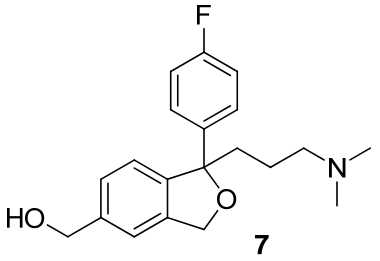

7

1.99 2.79 1.95 0.93 1.18 2.01 2.00 8.25 1.23 1.35

7.0 6.0 5.0 4.0 3.0 2.0

ppm (t1)

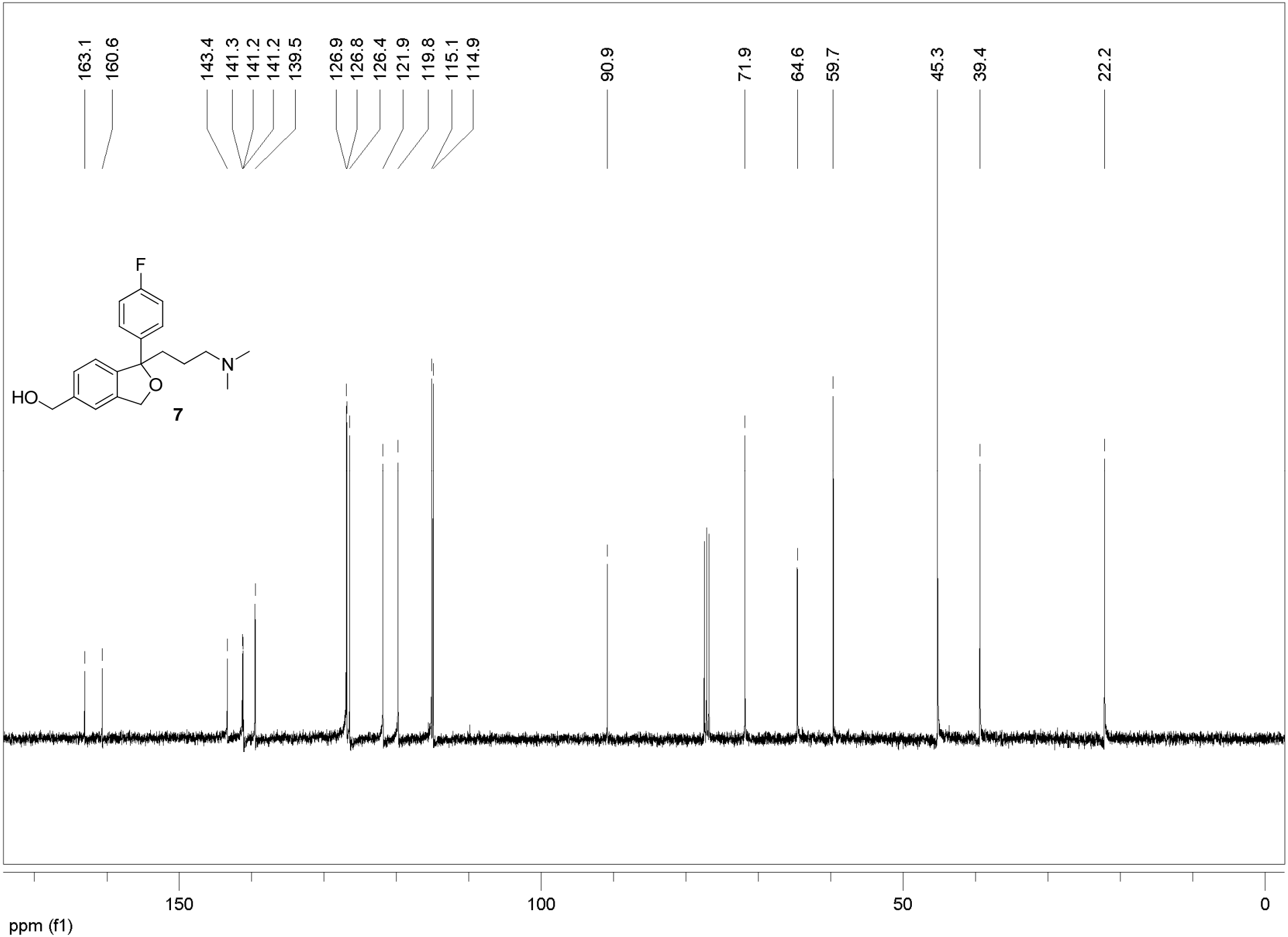
163.1
160.6
143.4
141.3
141.2
141.2
139.5
126.9
126.8
126.4
121.9
119.8
115.1
114.9
90.9
71.9
64.6
59.7
45.3
39.4
22.2
F
N
O
HO
7
150
100
50
0
ppm (f1)

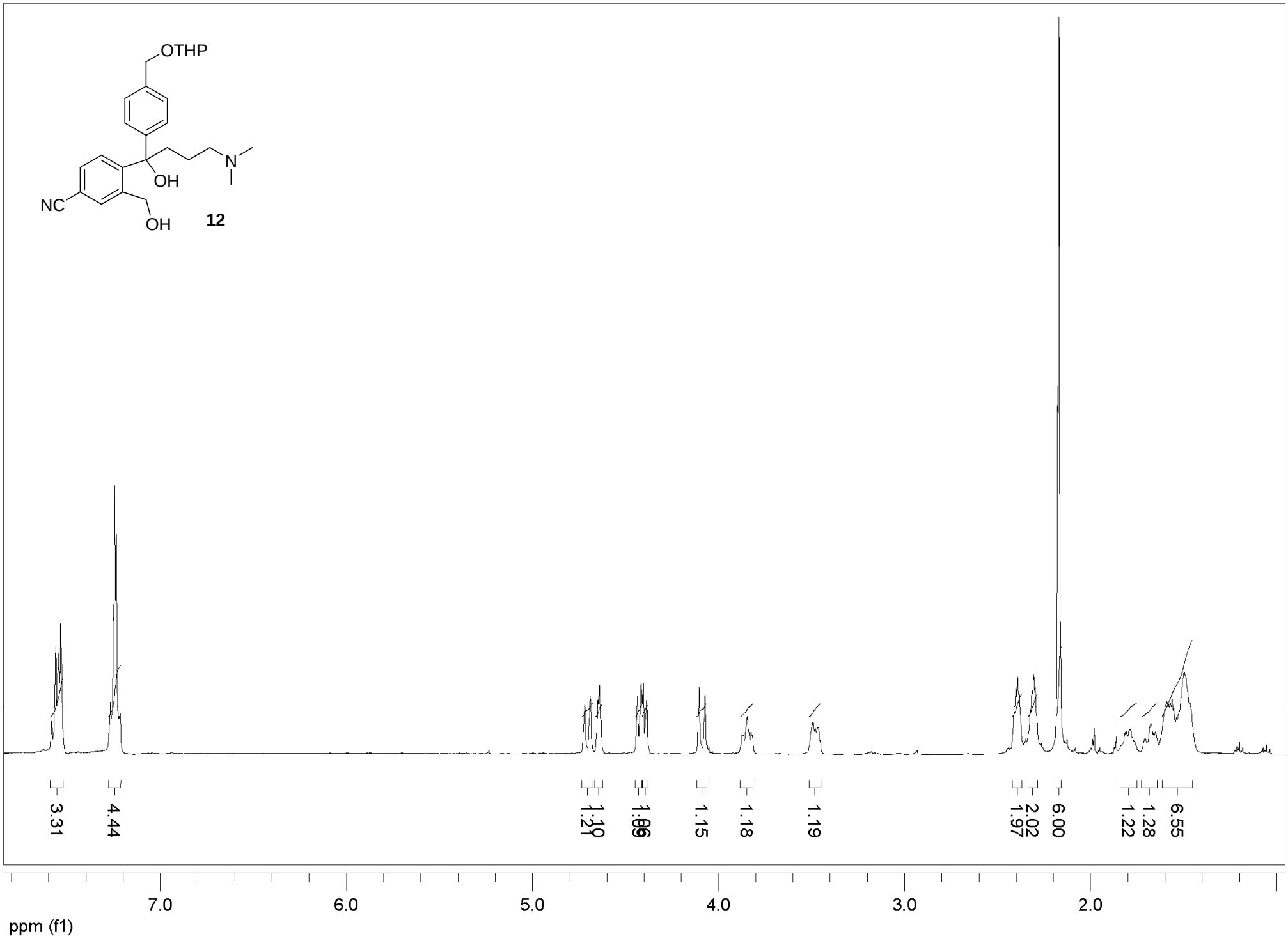
OTHP
OH
N
NC
OH
12
3.31
4.44
1.21
1.10
1.06
1.15
1.18
1.19
1.97
2.02
6.00
1.22
1.28
6.55
7.0
6.0
5.0
4.0
3.0
2.0
ppm (f1)

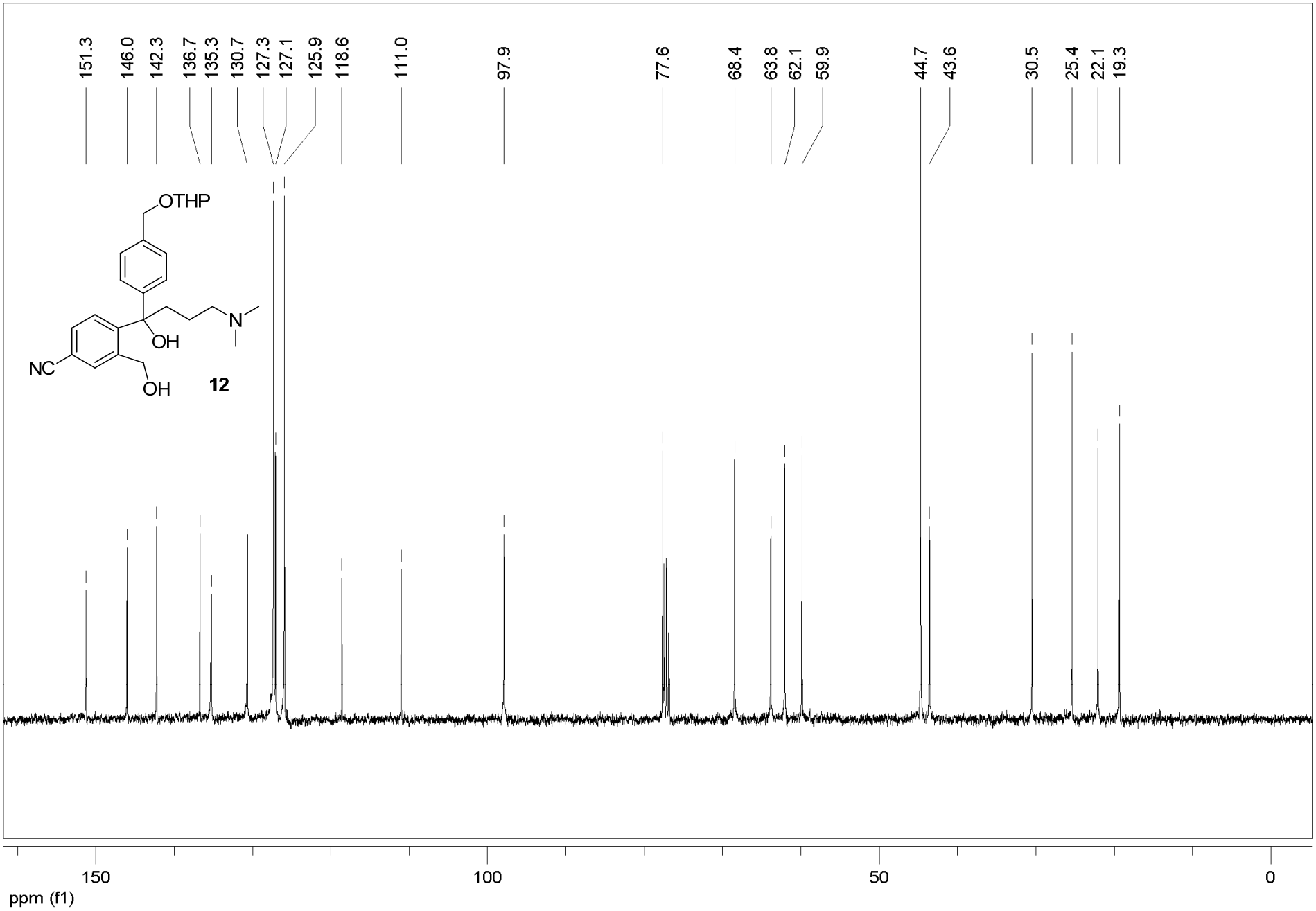
151.3
146.0
142.3
136.7
135.3
130.7
127.3
127.1
125.9
118.6
111.0
97.9
77.6
68.4
63.8
62.1
59.9
44.7
43.6
30.5
25.4
22.1
19.3
OTHP
N
OH
NC
OH
12
150
100
50
0
ppm (f1)

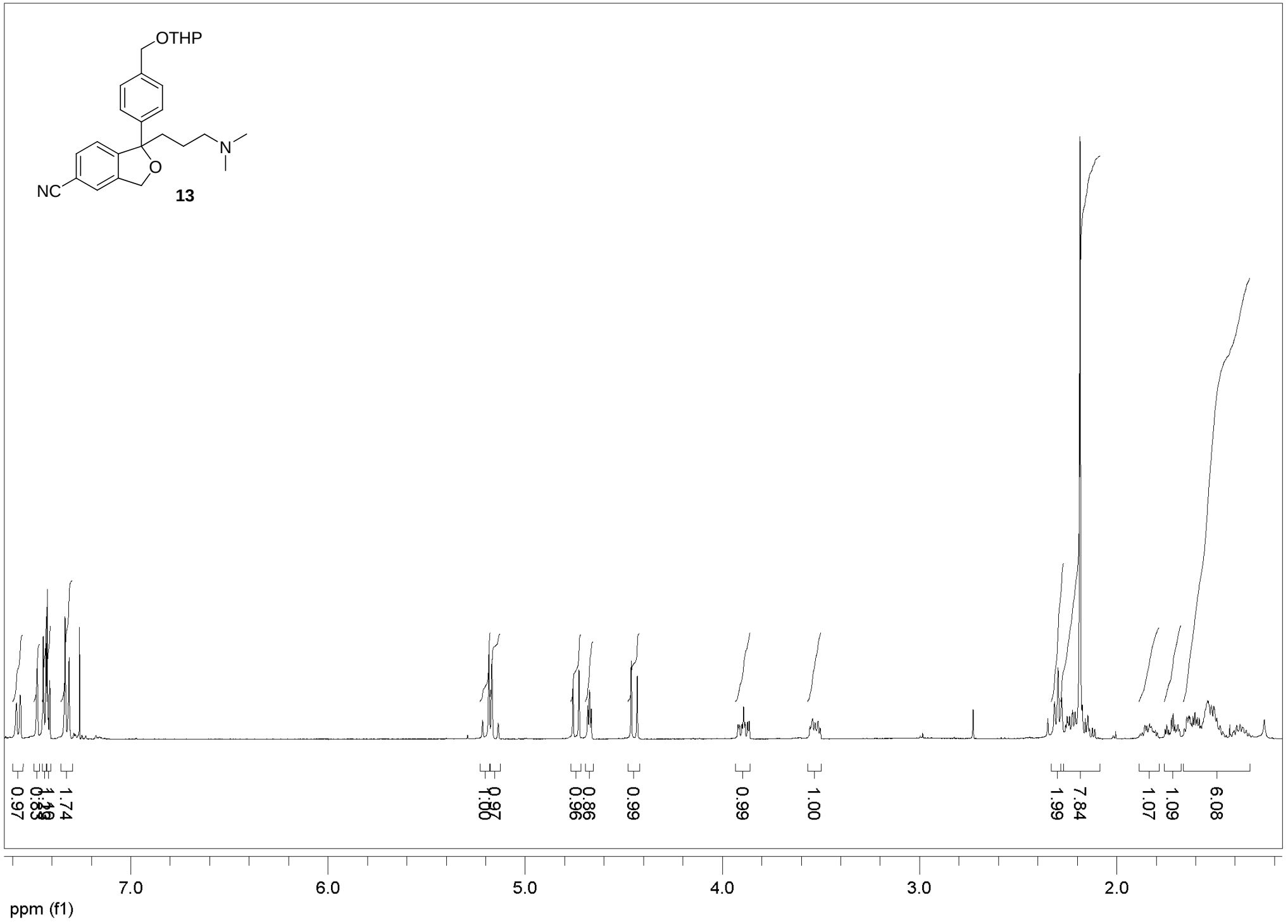
OTHP
N
O
NC
13
0.97
1.74
1.00
0.97
0.96
0.86
0.99
0.99
1.00
1.99
7.84
1.07
1.09
6.08
7.0
6.0
5.0
4.0
3.0
2.0
ppm (f1)

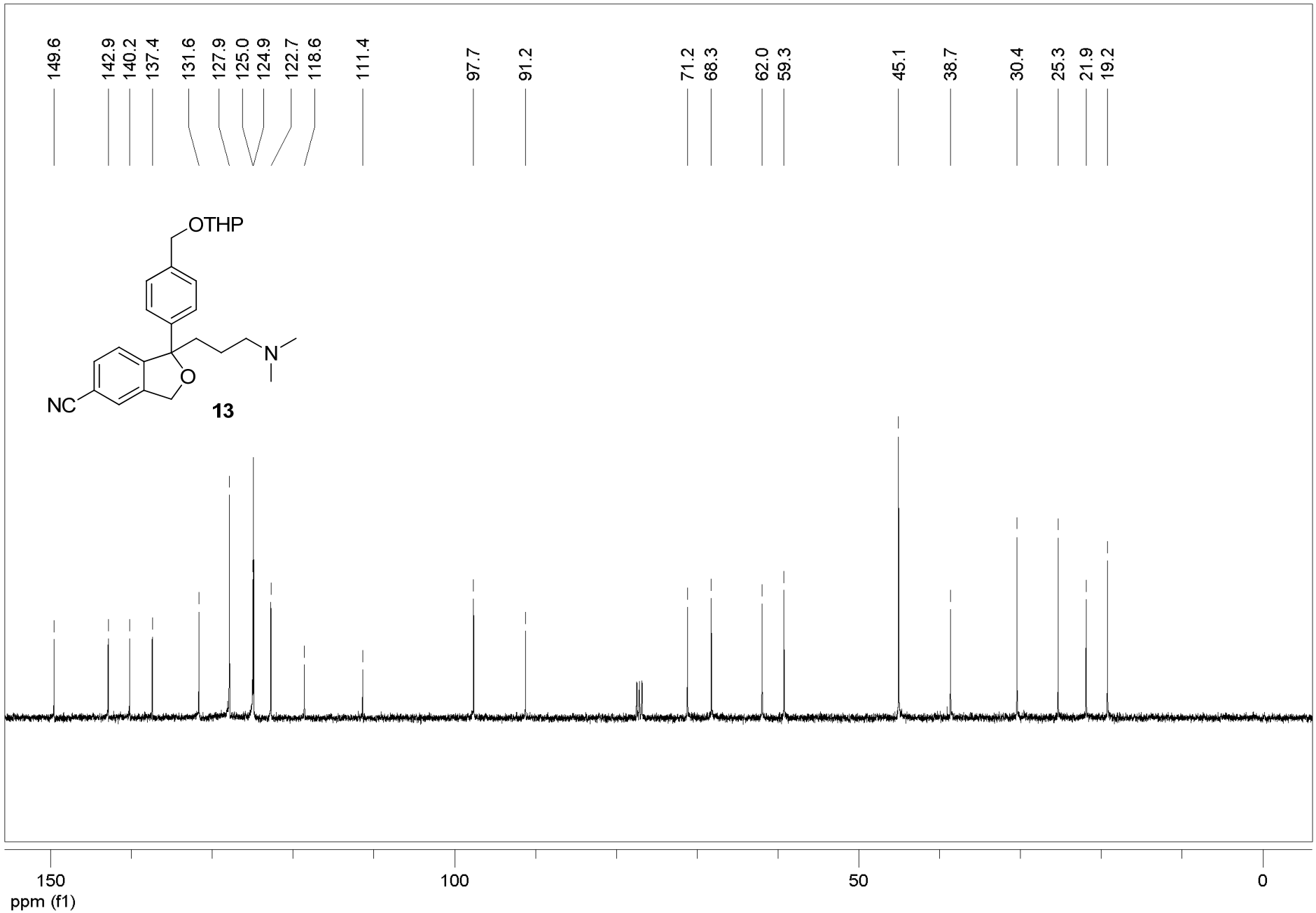
149.6
142.9
140.2
137.4
131.6
127.9
125.0
124.9
122.7
118.6
111.4
97.7
91.2
71.2
68.3
62.0
59.3
45.1
38.7
30.4
25.3
21.9
19.2
OTHP
N
O
NC
13
150
100
50
0
ppm (f1)

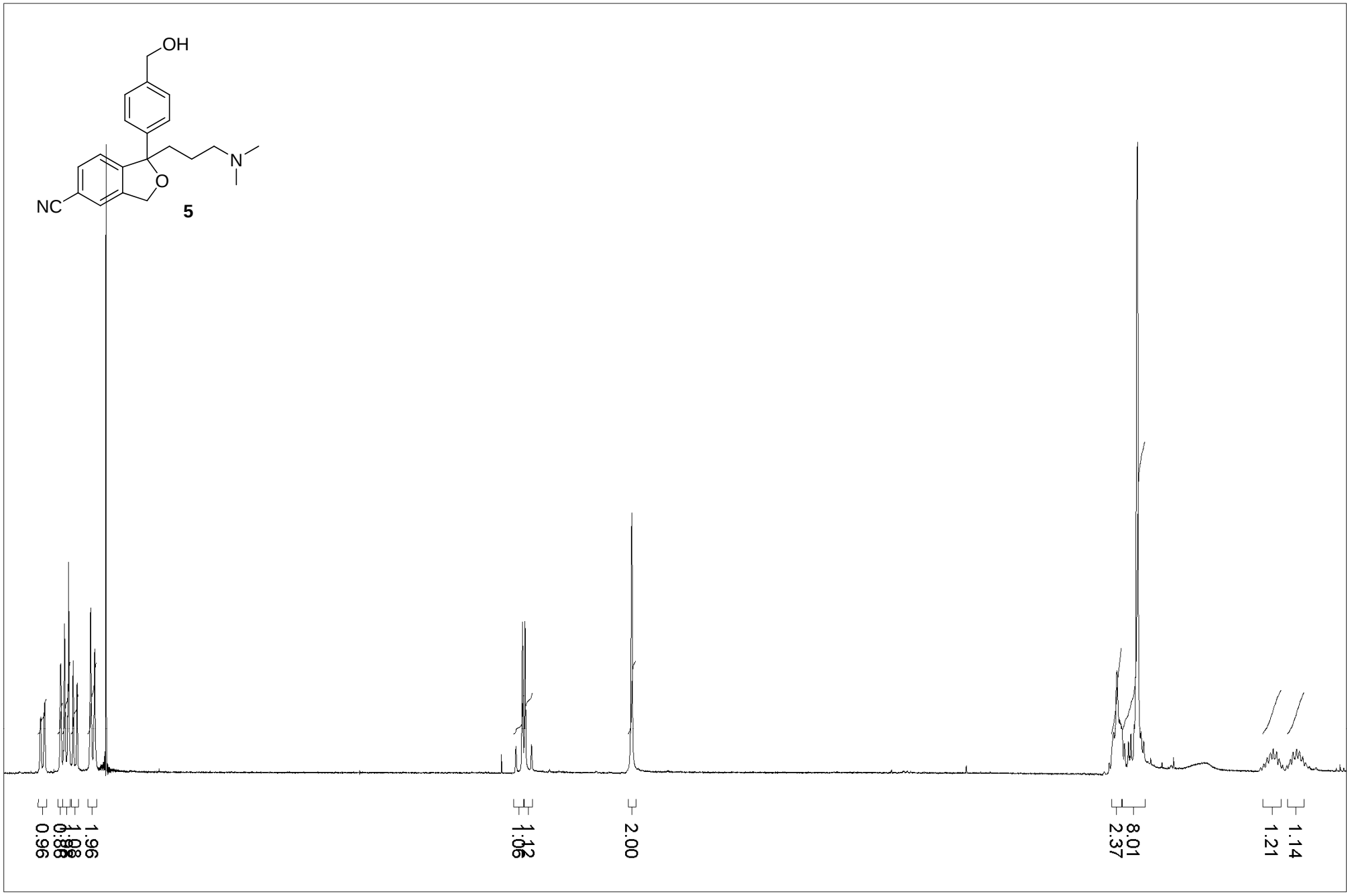
OH
N
O
NC
5
0.96
1.96
1.06
2.00
2.37
8.01
1.21
1.14
7.0
6.0
5.0
4.0
3.0
2.0
ppm (f1)

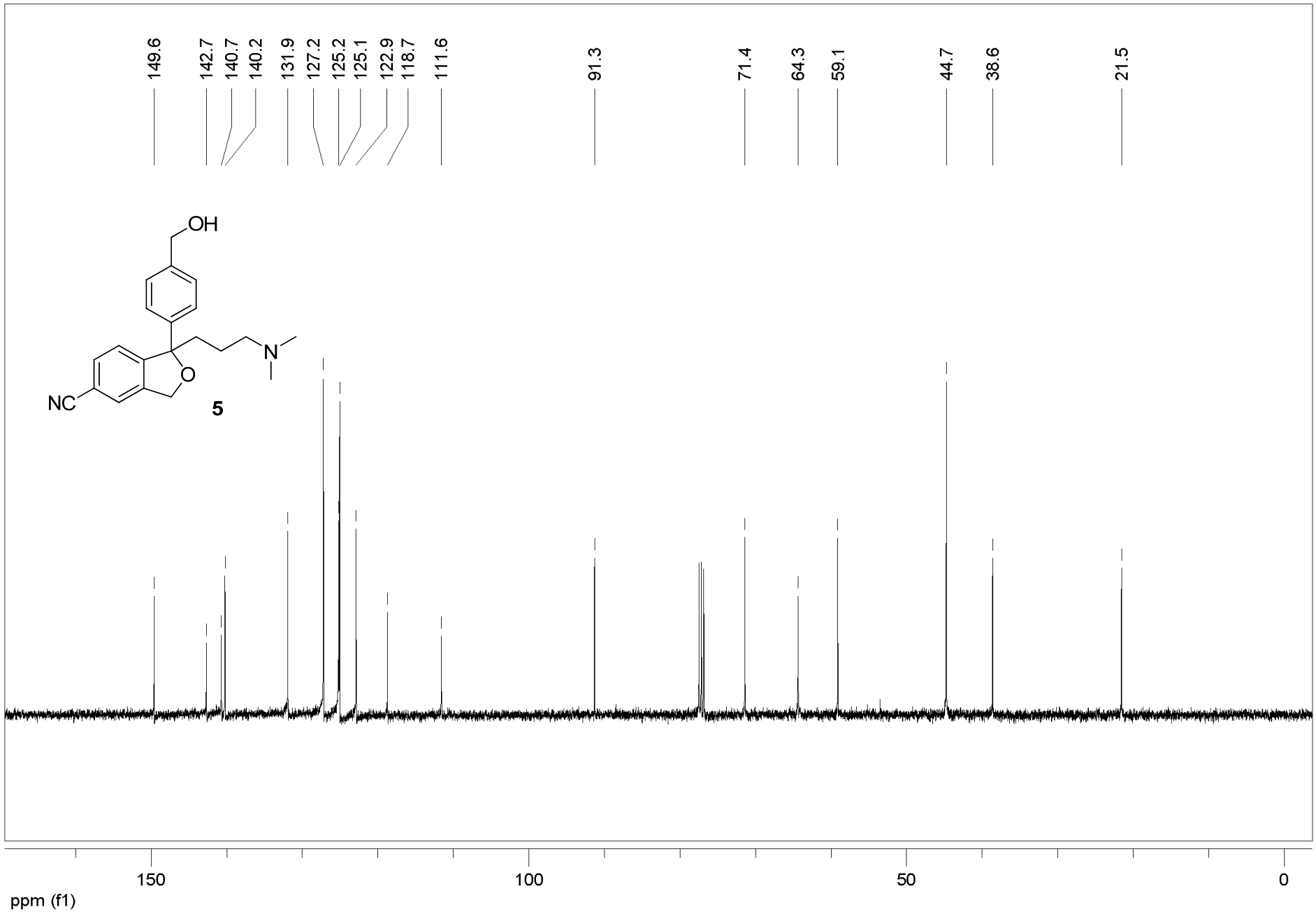
149.6
142.7
140.7
140.2
131.9
127.2
125.2
125.1
122.9
118.7
111.6
91.3
71.4
64.3
59.1
44.7
38.6
21.5
OH
N
O
NC
5
150
100
50
0
ppm (f1)

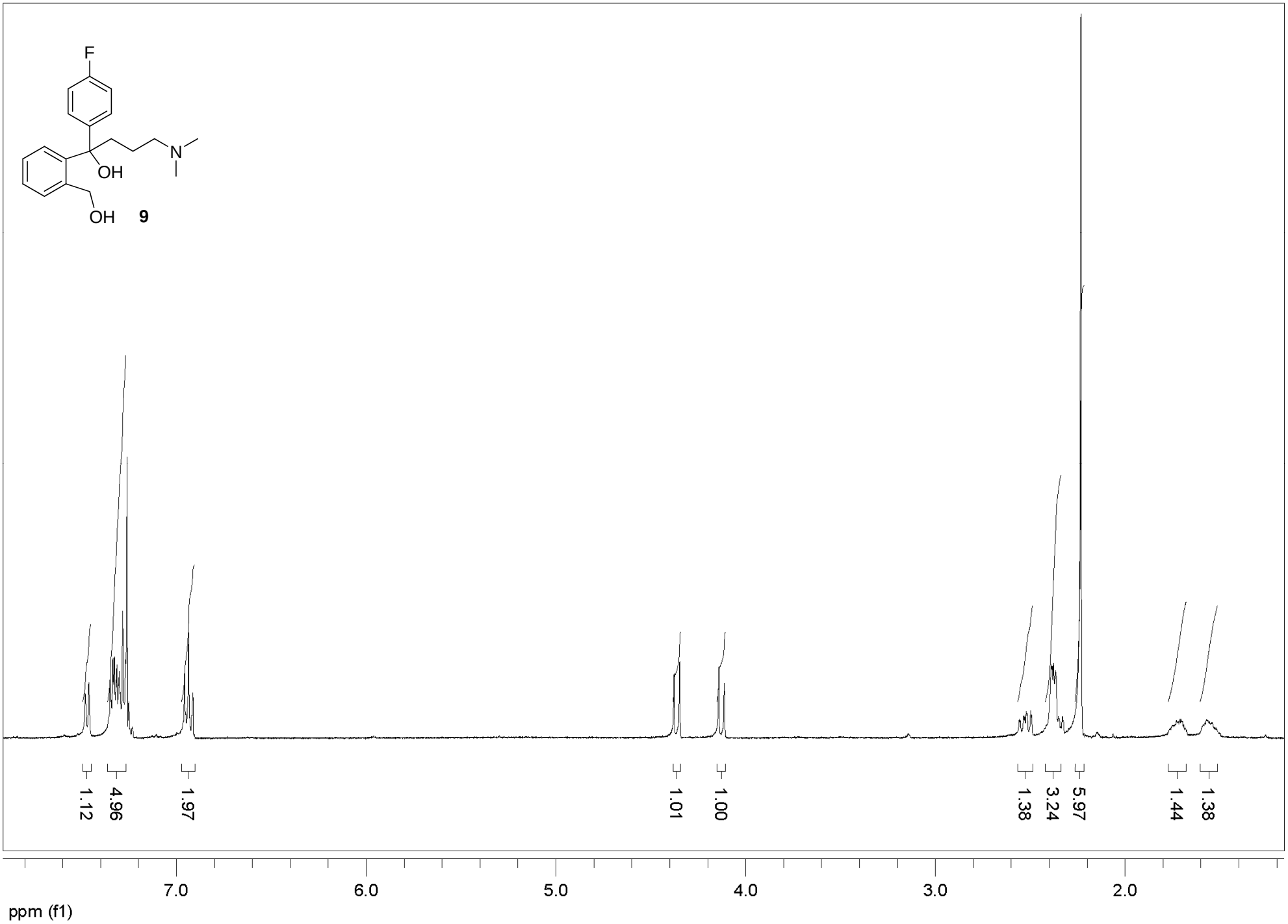
F
OH
N
OH
9
1.12
4.96
1.97
1.01
1.00
1.38
3.24
5.97
1.44
1.38
7.0
6.0
5.0
4.0
3.0
2.0
ppm (f1)

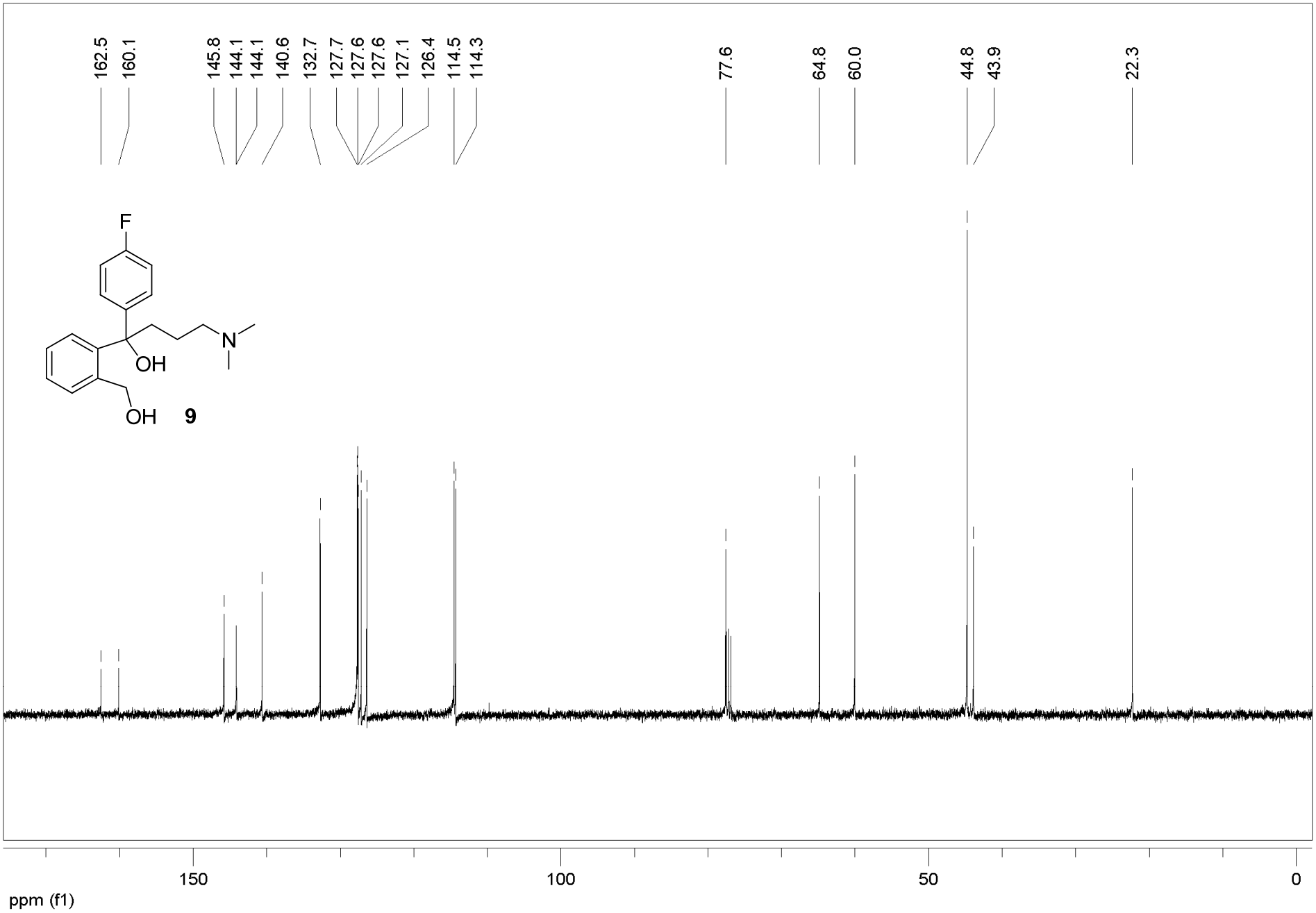
162.5
160.1
145.8
144.1
144.1
140.6
132.7
127.7
127.6
127.6
127.1
126.4
114.5
114.3
77.6
64.8
60.0
44.8
43.9
22.3
F
N
OH
OH
9
150
100
50
0
ppm (f1)

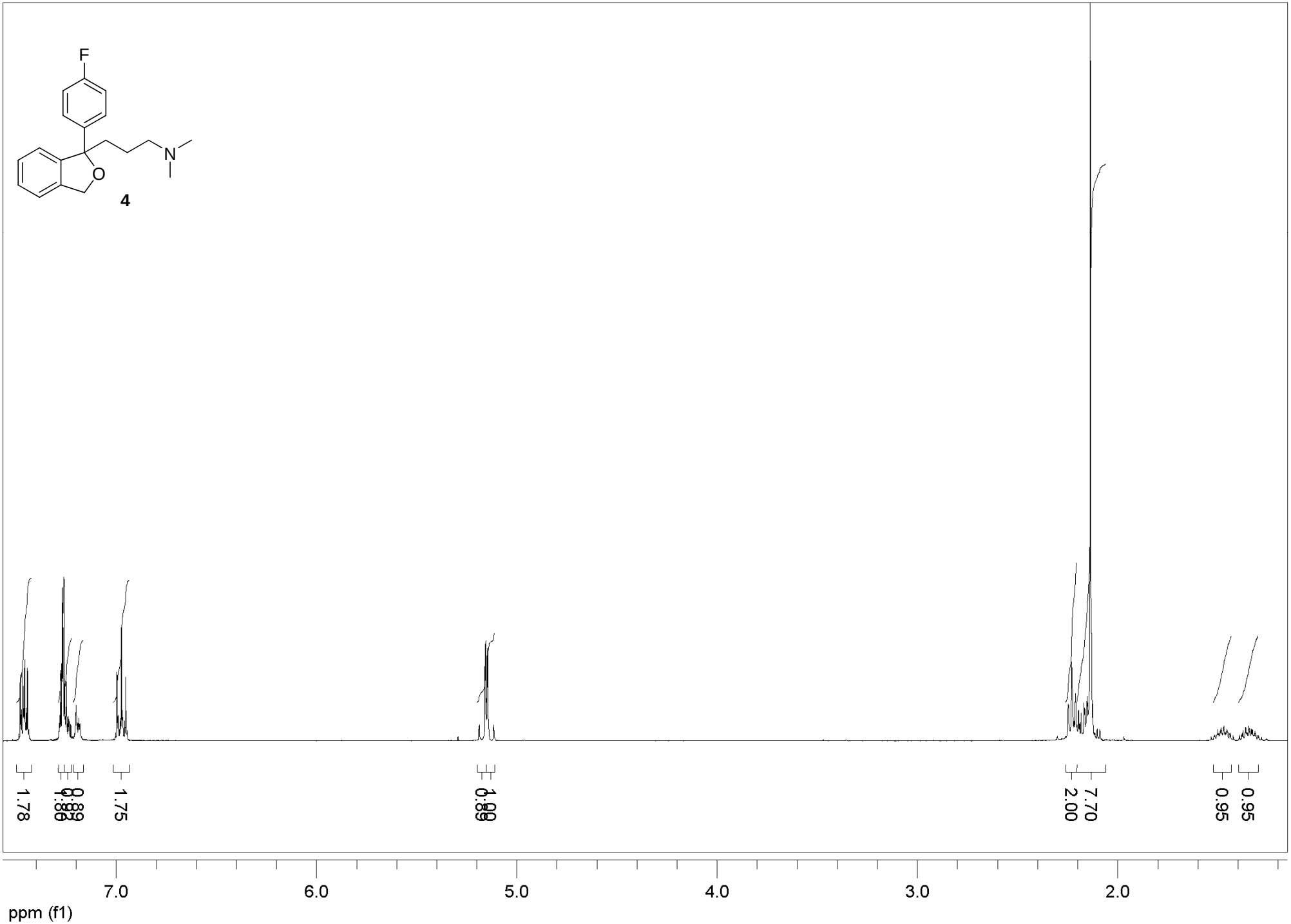
F
N
O
4
1.78
1.86
0.88
0.85
1.75
1.00
0.89
7.70
2.00
0.95
0.95
7.0
6.0
5.0
4.0
3.0
2.0
ppm (f1)

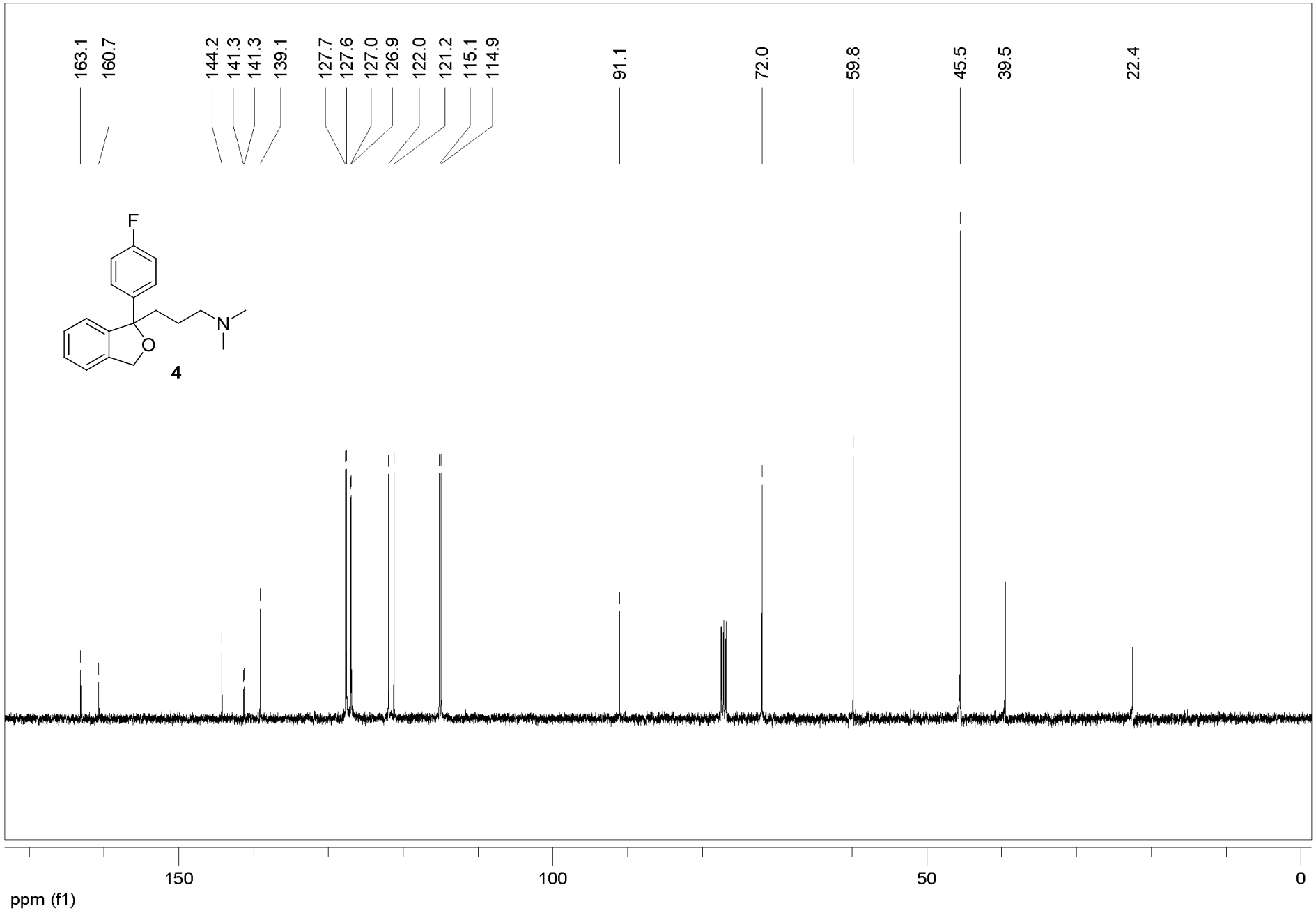
163.1
160.7
144.2
141.3
141.3
139.1
127.7
127.6
127.0
126.9
122.0
121.2
115.1
114.9
91.1
72.0
59.8
45.5
39.5
22.4
F
N
O
4
150
100
50
0
ppm (f1)

References

(1) Celik, L.; Sinning, S.; Severinsen, K.; Hansen, C.; Møller, M.; Bols, M.; Wiborg, O.; Schiøtt, B. *J. Am. Chem. Soc.* **2008**, *130*, 3853-3865.

(2) Yamashita, A.; Singh, S. K.; Kawate, T.; Jin, Y.; Gouaux, E. *Nature* **2005**, *437*, 215-223.

(3) Beuming, T.; Shi, L.; Javitch, J. A.; Weinstein, H. *Mol. Pharmacol.* **2006**, *70*, 1630-1642.

(4) Chen, J.; Liu-Chen, S.; Rudnick, G. *Biochemistry* **1997**, *36*, 1479-1486.

(5) Chen, R.; Wei, H.; Hill, E.; Chen, L.; Jiang, L.; Han, D.; Gu, H. *Mol. Cell. Biochem.* **2007**, *298*, 41-48.

(6) Cole, C.; Barber, J. D.; Barton, G. J. *Nucl. Acids Res.* **2008**, *36*, W197-201.

(7) McGuffin, L. J.; Bryson, K.; Jones, D. T. *Bioinformatics* **2000**, *16*, 404-405.

(8) Tate, C. G.; Blakely, R. D. *J. Biol. Chem.* **1994**, *269*, 26303-26310.

(9) Gaffaney, J. D.; Vaughan, R. A. *Mol. Pharmacol.* **2004**, *65*, 692-701.

(10) Sali, A.; Blundell, T. L. *J. Mol. Biol.* **1993**, *234*, 779-815.

(11) Fiser, A.; Do, R. K.; Scaronali, A. *Prot. Sci.* **2000**, *9*, 1753-1773.

(12) Eswar, N.; John, B.; Mirkovic, N.; Fiser, A.; Ilyin, V. A.; Pieper, U.; Stuart, A. C.; Marti-Renom, M. A.; Madhusudhan, M. S.; Yerkovich, B.; Sali, A. *Nucl. Acids Res.* **2003**, *31*, 3375-3380.

(13) Laskowski, R. A.; MacArthur, M. W.; Moss, D. S.; Thornton, J. M. *J. Appl. Cryst.* **1993**, *26*, 283-291.

(14) Luthy, R.; Bowie, J. U.; Eisenberg, D. *Nature* **1992**, *356*, 83-85.

(15) Bowie, J. U.; Luthy, R.; Eisenberg, D. *Science* **1991**, *253*, 164-170.

(16) Prime, version 2.0, Schrödinger, LLC, New York, NY, **2008**.

(17) www.molegro.com, Molegro Virtual Docker, version MVD2008.2.4.

(18) Thomsen, R.; Christensen, M. H. *J. Med. Chem.* **2006**, *49*, 3315-3321.

(19) Jørgensen, A. M.; Tagmose, L.; Jørgensen, A. M. M.; Topiol, S.; Sabio, M.; Gundertofte, K.; Bøgesø, K. P.; Peters, G. H. *ChemMedChem* **2007**, *2*, 815-826.

(20) Forrest, L. R.; Tavoulari, S.; Zhang, Y. W.; Rudnick, G.; Honig, B. *Proc. Natl. Acad. Sci. USA* **2007**, *104*, 12761-12766.

(21) Zomot, E.; Bendahan, A.; Quick, M.; Zhao, Y.; Javitch, J.; Kanner, B. *Nature* **2007**, *449*, 726-730.

(22) Kalé, L.; Skeel, R.; Bhandarkar, M.; Brunner, R.; Gursoy, A.; Krawetz, N.; Phillips, J.; Shinozaki, A.; Varadarajan, K.; Schulten, K. *J. Comp. Phys.* **1999**, *151*, 283-312.

(23) MacKerell, A. D. Jr., et al *J. Phys. Chem. B* **1998**, *102*, 3586-3616.

(24) MacKerell, A. D. Jr.; Feig, M.; Brooks, C. L. I. *J. Comput. Chem.* **2004**, *25*, 1400-1415.

(25) MacKerell, A. D. Jr.; Feig, M.; Brooks, C. L. I. *J. Am. Chem. Soc.* **2004**, *126*, 698-699.

(26) Maestro, version 7.5, Schrödinger, LLC, New York, NY, **2005**.

(27) Kaminski, G. A.; Friesner, R. A.; Tirado-Rives, J.; Jorgensen, W. L. *J. Phys. Chem. B* **2001**, *105*, 6474-6487.

(28) MacroModel, version 9.1, Schrödinger, LLC, New York, NY, **2005**.

(29) Boström, J.; Norrby, P.; Liljefors, T. *J. Comp. Aided Mol. Des.* **1998**, *12*, 383-383.

(30) Epik, version 1.6, Schrödinger, LLC, New York, NY, **2008**.

(31) Li, H.; Robertson, A. D.; Jensen, J. H. *Proteins: Structure, Function, and Bioinformatics* **2005**, *61*, 704-721.

(32) Glide, version 5.0, Schrödinger, LLC, New York, NY, **2008**.

(33) Schrödinger Suite 2008 Induced Fit Docking protocol; Glide version 5.0, Schrödinger, LLC, New York, NY, 2005; Prime version 1.7, Schrödinger, LLC, New York, NY, **2005**.

(34) Sherman, W.; Day, T.; Jacobson, M. P.; Friesner, R. A.; Farid, R. *J. Med. Chem.* **2006**, *49*, 534-553.

(35) Sinning, S.; Musgaard, M.; Jensen, M.; Severinsen, K.; Celik, L.; Koldsø, H.; Meyer, T.; Bols, M.; Jensen, H. H.; Schiøtt, B.; Wiborg, O. *J. Biol. . Chem.* **2009**, *doi:10.1074/jbc.M109.045401*.

(36) Larsen, M. B.; Elfving, B.; Wiborg, O. *J. Biol. Chem.* **2004**, *279*, 42147-42156.

(37) Henry, L. K.; Field, J. R.; Adkins, E. M.; Parnas, M. L.; Vaughan, R. A.; Zou, M. F.; Newman, A. H.; Blakely, R. D. *J. Biol. Chem.* **2006**, *281*, 2012-2023.

(38) Barker, E. L.; Moore, K. R.; Rakhshan, F.; Blakely, R. D. *J. Neurosci.* **1999**, *19*, 4705-4717.

(39) Chen, J.; Sachpatzidis, A.; Rudnick, G. *J. Biol. Chem.* **1997**, *272*, 28321-28327.

(40) Mortensen, O. V.; Kristensen, A. S.; Wiborg, O. *J. Neurochem.* **2001**, *79*, 237-247.

(41) Friesner, R. A.; Banks, J. L.; Murphy, R. B.; Halgren, T. A.; Klicic, J. J.; Mainz, D. T.; Repasky, M. P.; Knoll, E. H.; Shelley, M.; Perry, J. K.; Shaw, D. E.; Francis, P.; Shenkin, P. S. *J. Med. Chem.* **2004**, *47*, 1739-1749.

(42) Friesner, R. A.; Murphy, R. B.; Repasky, M. P.; Frye, L. L.; Greenwood, J. R.; Halgren, T. A.; Sanschagrin, P. C.; Mainz, D. T. *J. Med. Chem.* **2006**, *49*, 6177-6196.

(43) Schrödinger Suite 2008 QM-Polarized Ligand Docking protocol; Glide version 5.0, Schrödinger, LLC, New York, NY, 2008; Jaguar version 7.5, Schrödinger, LLC, New York, NY, 2008; QSite version 5.0, Schrödinger, LLC, New York, NY, **2008**.

(44) Cho, A. E.; Guallar, V.; Berne, B. J.; Friesner, R. *J. Comput. Chem.* **2005**, *26*, 915-931.

(45) Murphy, R. B.; Philipp, D. M.; Friesner, R. A. *J. Comput. Chem.* **2000**, *21*, 1442-1457.

(46) MacroModel, version 9.6, Schrödinger, LLC, New York, NY, **2008**.

(47) http://www.moldiscovery.com/soft_grid.php.

(48) Lin, H. -S.; Paquette, L. A. *Synth. Comm.* **1994**, *24*, 2503-2506.

(49) Kobayashi, Y.; Tokoro, Y.; Watatani, K. *Eur. J. Org. Chem* **2000**, *2000*, 3825-3834.